CATALYTIC VAPOUR PHASE CONDENSATION OF METHANOL AND ANILINE TO DIMETHYLANILINE

VERIFIED
INL ....

A THESIS

SUBMITTED TO

THE UNIVERSITY OF BOMBAY

FOR THE DEGREE OF

MASTER OF SCIENCE (TECHNOLOGY)

COMPUTERISED

BY

KRISHAN KIRTI VERMA,

B.Sc., B.Sc. (Tech.)

NATIONAL CHEMICAL LABORATORY

POONA 8

MARCH 1964

0413: 54197
VER

TH-746

VERIFIED
1977
INL ....

NATIONAL CHEMICAL LABORATORY
4464
LIBRARY

ACKNOWLEDGEMENT

I am deeply indebted to Dr. L.K.Doraiswamy, Assistant Director, National Chemical Laboratory, Poona, for his inspiring guidance during the pursuit of this investigation.

I am also indebted to my colleagues for the encouragement and suggestions given by them while carrying out this work.

My thanks are also due to the Council of Scientific and Industrial Research for the award of a Junior Research Fellowship to me during the period of this work. I am also thankful to The University of Bombay for the award of "Shri Khushiram Wadhumal Khubchandani" merit scholarship.

COMPUTERISED

Kishan Kumar Verma

(K.K.Verma)

National Chemical Laboratory,
Poona 8.

C O N T E N T S

CHAPTER - 1

SUMMARY

Dimethylaniline is a commercially important intermediate for the manufacture of basic dyes and pharmaceutical products. It also finds use in the ammunition industry for the manufacture of tetryl, a booster in all types of grenades, and allied products.

There are broadly two methods by which dimethylaniline can be produced : (1) liquid phase reaction between aniline and methyl alcohol in the presence of sulphuric acid; and (2) vapour phase methylation of aniline (with methanol or dimethyl ether) over a solid dehydrating catalyst. For liquid phase methylation of aniline to dimethylaniline, literature survey has revealed that in place of sulphuric acid, other catalysts such as methyl bromide and boron trifluoride can stan be employed. Vapour phase methylation of aniline to dimethylaniline has several advantages. It is a process which can be made continuous easily, and can be operated at atmospheric pressure. Several patents have been taken on the use of a variety of dehydrating catalysts for this reaction, but alumina is claimed to be the best.

The objectives of the present investigation were as follows : (1) to make a complete thermodynamic analysis of the various reactions involved; (2) to obtain product distribution data for the vapour phase

methylation of aniline over a bauxite catalyst; and (3) to attempt a simple preliminary correlation of the data.

The thermodynamic properties of mono- and dimethylanilines are not available. These data have been calculated from available generalised procedures. Two principal reaction routes should be recognised for the formation of dimethylaniline from methanol and aniline : (1) aniline reacting directly with methanol to give mono- and dimethylanilines; and (2) dehydration of methanol to dimethyl ether which then reacts with aniline to give mono- and dimethylanilines. Several reactions are possible from these routes, and the thermodynamics of all these reactions have been quantitatively evaluated. The thermodynamic data revealed that the principal reactions involved are only slightly exothermic, and the heat of reaction for the main reaction (methanol and aniline going to dimethylaniline) is substantially independent of temperature.

The product distribution data were obtained in a glass integral reactor. Isothermal conditions could be attained in the reaction zone by using a thermostatic block of metal with a central hole for accommodating the reactor.

Process data were then obtained under such conditions that the effect of mass transfer was negligible. Reaction products were analysed by vapour phase

chromatography, and the product distribution plots showed expected trends. Assuming pseudo-first order kinetics, it has been possible to develop an equation for the high conversion range and to correlate the rate constants with temperature by the usual Arrhenius method. An empirical correlation of selectivity (with respect to dimethylaniline) as a function of conversion and temperature has also been possible.

CHAPTER - 2

LITERATURE REVIEW

The methylation of aniline to dimethylaniline (DMA) essentially proceeds according to the following scheme :

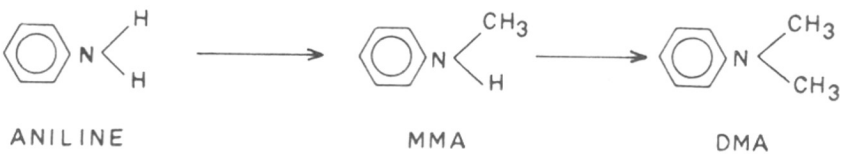

ANILINE MMA DMA

If the reaction conditions are not properly controlled, there is a possibility of ring methylation. Broadly the methods available for the preparation of DMA can be classified under two heads : (1) liquid phase methylation in the presence of acid or other suitable catalysts; and (2) vapour phase methylation using a suitable dehydrating catalyst.

Liquid phase methylation

DMA has been manufactured on a commercial scale by the liquid phase methylation of aniline since 1866[19]. As carried out industrially, 100 parts of aniline, 110 parts of methanol and 10 parts of 66° Be' sulphuric acid are charged into a steel autoclave and heated at 205° for 6 hours. The DMA thus produced should contain less than 1.0 per cent methylaniline[9].

A complete study of the process (using sulfuric acid as catalyst) has been made by Shreve and co-workers[21], who determined the effect of time, temperature, catalyst concentration, alcohol-amine ratio and free board on the rate of methylation of aniline. In place of sulfuric acid,

methyl bromide[6] and boron trifluoride[13] have also been used as catalysts.

Reductive methylation has also been employed for the production of DMA[18].

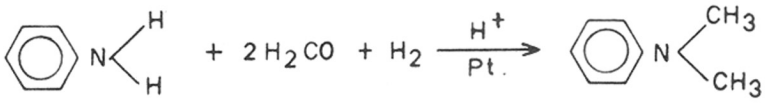

ANILINE DMA

A mixture of aniline hydrochloride, water, sulphuric acid and alcohol is cooled to 0° and charged to a hydrogenation apparatus over pre-reduced Adams catalyst along with trioxane, and hydrogenation is carried out at 45 psi total pressure. A yield of 72 per cent is claimed by this method.

Aniline has been methylated to DMA by refluxing it with trimethyl phosphate at 60° for 2 hours[2], and a yield of 67.9 per cent is reported.

A British patent[5] recommends the use of an iodide catalyst for the alkylation of aniline. It is also possible to alkylate salts of aniline or aniline metallic salt complexes under atmospheric pressure with aluminium alkoxide at considerably lower temperatures than those needed for aniline itself[4].

DMA can also be obtained by the direct replacement of the bromine atom of bromobenzene or the hydroxyl group of phenol by $-N(CH_3)_2$ at an elavated temperature using copper chloride as catalyst[12].

The liquid phase method has the following disadvantages :

(1) It is a batch reaction generating medium pressure.

(2) Caustic soda treatment is necessary before the distillation of the product.

(3) Considerable loss of methyl alcohol results from the formation of dimethyl ether, which escapes during the blow off at the end of the run.

Vapour phase methylation

The vapour phase methylation process essentially consists in passing a preheated mixture of aniline and excess methanol (or dimethyl ether) over a heated dehydrating catalyst. The vapours are condensed for the recovery of DMA and excess methylating agent is recycled.

Mailh and Godon[16] were the first to claim that by using alumina as catalyst, a mixture of mono- and dimethylanilines could be obtained at a temperature of about 430°.

Roy[20] used thoria supported on asbestos as catalyst, and obtained conversions of 67 and 75 per cent at 390° and 430° respectively.

A U.S. patent[14] claims hydrosilicates activated by treatment with mineral acid as good dehydrating catalysts for the production of DMA from methanol and aniline.

The use of alumina-molybdenum oxide catalyst has also been reported[10]. This was prepared by adding

ammonia solution to an acid mixture of aluminium chloride and ammonium molybdate to a pH of 8, the suspension was allowed to stand for a long time, and the solid was filtered off and washed until the product when dried contained less than 10 per cent ammonium chloride. This dried product was calcined at about 590° and was used in the form of pellets. A conversion of 45 per cent is claimed with a molar ratio of 1:2.5 and a temperature of 260°.

A variety of catalysts has been tried by Hill[11], who found aluminium oxide, thorium oxide and phosphoric acid to be the most active. Aluminium oxide, prepared artificially, is reported to be very efficient for side chain alkylation, but more nuclear alkylation was effected than anticipated. With alumina lumps, a conversion of 92 per cent is claimed at a space velocity of 100 reciprocal hours and a temperature of 360°.

Orthophosphoric acid deposited on crushed pumic is claimed[1] to give high conversions to DMA, using methanol and aniline vapours.

A process for obtaining DMA of a high degree of purity with a wet set point of 2° is claimed by a British patent[15]. Aniline and methanol are reacted in vapour phase at a temperature 200-230° in the presence of a catalyst containing precipitated alumina supported on calcined Indian bauxite. A better efficiency is claimed in the absence of air.

A pilot plant study of this process has been carried

out by Evans[7]. Both methyl alcohol and methyl ether have been used (separately) for methylation. It is claimed that by using methyl ether and aniline in the ratio of 5:1 over activated alumina at 275-285°, a quantitative yield of DMA can be obtained.

The complete process used at I.G.Ludwigshafen has been described in a FIAT report[8]. According to this method, DMA is produced catalytically by the reaction of aniline vapours with dimethyl ether over a contact mass of activated alumina between 230 and 295°. It is necessary to use a special type of highly reactive alumina catalyst, since splitting off of water proceeds only at relatively high temperatures with less reactive catalysts. Higher temperatures lead to side reactions, particularly ring methylation. The reaction is carried through in two steps and in two separate systems : (1) production of crude DMA containing 94-96 per cent DMA and 4-6 per cent methylaniline; and (2) further reaction of this crude DMA with dimethyl ether to give pure DMA. The reason for this division into two steps is the desire to methylate at temperatures as low as possible in order to avoid side products.

Passage of anisole and aniline vapours at 300° over aluminium oxide or synthetic aluminosilicate leads to the rupture of the Me-O bond and aniline is methylated to give DMA and MMA[3].

According to a U.S. patent[17], DMA can be produced

by passing aniline and methanol in the ratio of 1:2 through a column containing concentrated phosphoric acid at 180-200° in a yield of 92-95 per cent DMA. A second pass of the crude product through the catalyst bed, after stripping off the aqueous methanol and adding fresh methanol, is claimed to give 99 to 99.5 per cent conversion to DMA.

REFERENCES

1. Andrews, C.E., U.S.P. 2,073671 (March 16, 1937).
2. Billman, J.H., J. Am. Chem. Soc., 64, 2977 (1942).
3. Dobrovolskii, S.V. and Polotnyuk, V. ya., Zur. Obshchei. Khim., 27, 3191 (1957).
4. Earl, J.G., J. Chem. Soc., Part II, 973 (1947).
5. E.I. DU PONT DE Nemours & Co., B.P. 145,743 (July 2, 1920).
6. Edger, C.B. and Williams, H., U.S.P. 1,794,057 (February 24, 1931).
7. Evan, T.H., Canadian J. Tech., 29, 1, (1951).
8. FIAT Report No. 1313, Vol. I, p417.
9. Groggins, P.H. "Unit Processes in Organic Synthesis," (McGraw-Hill Inc., New York, 5th ed., 1958), p850.
10. Howard, P.H., U.S.P. 2,565,428 (August 21, 1951).
11. Hill, A.G., Ind. Eng. Chem., 43, 1579 (1951).
12. Imperial Chemical Industries, G.P. 564436 (May 20, 1931).
13. Joseph, B.D. and James, G.M., U.S.P. 2,391,139 (December 18, 1945).
14. Karl, S., U.S.P. 1,908,190 (May 9, 1932).
15. Maxted, E.B., B.P. 577,901 (March 10, 1944).
16. Mailhe, F. de Godon, Compt. Rend., 166, 467 (1918).
17. Matthias, T., U.S.P. 2,991,311 (November 26, 1958).
18. Pearson, D.E. and Briton, J.D., J. Am. Chem. Soc., 73, 864 (1951).
19. Poirrier and Chappat, Bull. Soc. Chim., 6, 502 (1866).
20. Roy, B.C., J. Ind. Chem. Soc., 5, 383 (1928).
21. Shreve, R.N., Vriens, G.M., and Vogel, A., Ind. Eng. Chem., 42, 791 (1950).

CHAPTER - 3

THERMODYNAMIC CONSIDERATION

Several reactions are possible under the conditions normally employed for the condensation reactions leading to the formation of mono- and dimethylanilines.

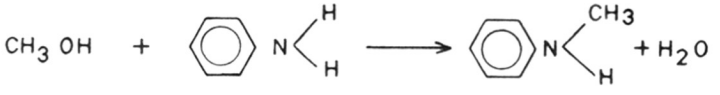

(i)

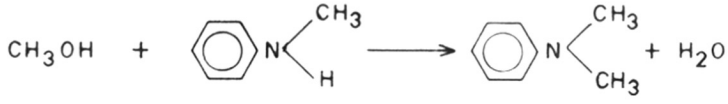

(ii)

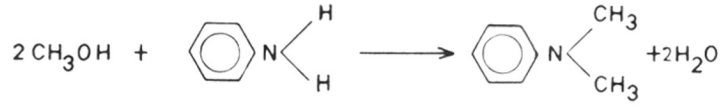

(iii)

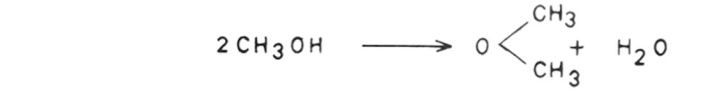

(iv)

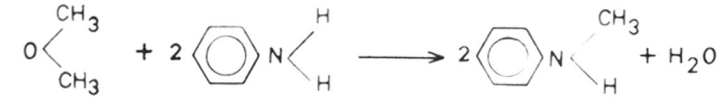

(v)

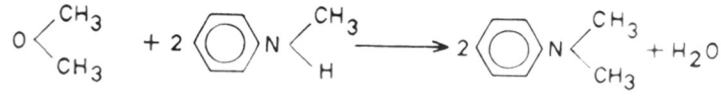

(vi)

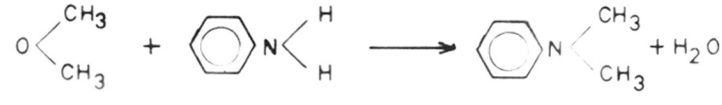

(vii)

The ultimate mechanism by which MMA and DMA are formed will depend upon the relative rates of these reactions. But in this chapter attention will be restricted to the thermodynamic feasibility of each of these reactions. Quantitative evaluation of these reactions will also be made, using available thermodynamic data where possible and estimated values where necessary. Before undertaking such a study, a brief summary will be given of the thermodynamic properties of each of the components of these reactions.

Aniline

The thermodynamic properties of aniline have recently been calculated[7] from the spectroscopic data of Evans[4]. These properties are summarised in Table-1.

Methanol

The thermodynamic properties of methanol reported by Green[6] are listed in Table-2. The values of ΔG°_f and log K_f were checked by the following procedure. ΔG°_f was calculated from the equation,

$$\frac{\Delta G^\circ_T}{T} = \left[\frac{G^\circ_T - H^\circ_o}{T} + \frac{\Delta H^\circ_{f_o}}{T}\right]_C - \lesssim \left[\frac{G^\circ_T - H^\circ_o}{T}\right]_E \qquad (1)$$

using the values of the function $\frac{G^\circ_T - H^\circ_o}{T}$ for methanol

and its constituent elements[9]. The value of $\Delta H^\circ_{f_\circ}$ was estimated from the heat of formation at 298°K using Equation (2) :

$$\Delta H^\circ_{f_T} = \Delta H^\circ_{f_\circ} + (H^\circ_T - H^\circ_\circ)_C - \lesssim (H^\circ_T - H^\circ_\circ)_E \qquad (2)$$

The equilibrium constants of formation were then calculated from the relation,

$$\frac{\Delta G^\circ_f}{T} = -R \ln K \qquad (3)$$

The estimated values of ΔG°_f and log K_f agreed quantitatively [Table-2] with those reported by Green[10].

Dimethyl ether

The principal thermodynamic functions of dimethyl ether have been calculated by Banerjee and Doraiswamy[1], but these authors did not include the values of ΔG°_f, ΔH°_f and log K_f. ΔG°_f was calculated from Equations (1) and (2) and log K_f from Equation (3), as described earlier. The thermodynamic functions of dimethyl ether appear in Table-4.

Monomethylaniline

In the case of monomethylaniline none of the thermodynamic functions have been reported. All the values were therefore estimated from available generalised procedures.

Heat capacity :

The heat capacity was calculated from the equation,

$$C_P^\circ = 4R + \frac{aR}{2} + \Sigma q_i C_{vi} + \frac{(3n - 6 - a - \Sigma q_i)}{\Sigma q_i} \times \Sigma q_i C_{\delta i} \qquad (5)$$

recommended by Dobratz[3]. In using this equation the following values may be noted :

Number of atoms in the molecule (n)	=	17
Number of bonds permitting free rotation (a)	=	2
Number of bonds in the molecule(Σq_i)	=	17

Based on the fundamental bond frequency assignments of Bennewitz and Rossner[2] and Stull and Mayfield[10], Hougen and Watson[13] have plotted C_v and C_δ as functions of temperature for various frequencies (wave numbers). Using this chart, heat capacity has been calculated as a function of temperature. These values are summarised in Table-5 and plotted in Fig. (1). The following equation was then developed by the method of least squares :

$$C_P^\circ = -1{\cdot}1536 + 11{\cdot}4115 \times 10^{-2} T - 0{\cdot}48904 \times 10^{-4} \times T^2 + 0{\cdot}0061883 \times 10^{-6} \times T^3 \qquad (6)$$

Heat capacities calculated from this equation are plotted in Fig. (1) to indicate the accuracy of the proposed equation in the temperature range 300-1500°K. The equation

holds good to within 2 per cent.

Recently another method based on group contributions has been proposed by Rihani and Doraiswamy[8]. According to this procedure the values of the constants a, b, c, d for any organic compound can be estimated from the values for the constituent groups and bonds. The equation developed by this method is :

$$C_P^\circ = -9.3186 + 15.4259 \times 10^{-2} \times T - 0.9689 \times 10^{-4} \times T^2 + 0.02295 \times 10^{-6} \times T^3 \quad (7)$$

The values calculated from Equation (7) are also plotted in Fig. (1).

Heat of formation :

The heat of formation was calculated by an indirect method. The heat of reaction at different temperatures for the reaction

$$\text{ANILINE} + \text{METHANOL} \longrightarrow \text{MMA} + \text{WATER} \quad (i)$$

was first calculated from the C_p^o equations for the constituents and the heat of reaction (ΔH_r°) value at 298^oK[12]. Then, from the values of ΔH_r° and ΔH_f° of aniline, methanol and water at different temperatures, ΔH_f° for MMA was calculated as a function of temperature. These values are listed in Table-5.

Free energy of formation :

Values of free energy of formation in the range 300-1500°K were calculated by van Krevelan's method[11]. The following two equations were developed for ΔG_f° as a function of temperature :

Range 300-600°K.

$$\Delta G_f^\circ = 21{\cdot}897 + 9{\cdot}600 \times 10^{-2} T \qquad (8)$$

Range 600-1500°K.

$$\Delta G_f^\circ = 18{\cdot}155 + 10{\cdot}114 \times 10^{-2} T \qquad (9)$$

A plot of ΔG_f° Vs T in the range 300-1500°K is shown in Fig. (3), and the values are summarised in Table-5.

Entropy :

The entropy change of reaction (i) was first calculated from the equation

$$\Delta S_r^\circ = \frac{-\Delta G_r^\circ + \Delta H_r^\circ}{T} \qquad (10)$$

from a knowledge of ΔG_r° and ΔH_r°. The absolute entropy of MMA was then computed from the relationship,

$$\Delta S_r^\circ = S^\circ_{MMA} + S^\circ_{H_2O} - S^\circ_{MeOH} - S^\circ_{A} \qquad (11)$$

The estimated figures are listed in Table-5.

log K_f :

As in the case of methanol and dimethyl ether, log K_f was computed from Equation (3). The estimated figures are listed in Table-5.

Dimethylaniline

In the case of dimethylaniline, none of the thermodynamic functions has been reported. All the values have therefore been estimated from available generalised procedures.

Heat capacity :

The heat capacity was calculated from Equation (5). In using this equation, the following values may be noted.

Number of atoms in the molecule (n)	=	20
Number of bonds permitting free rotation (a)	=	3
Number of bonds in the molecule (Σq_i)	=	20

Using the chart of Hougen and Watson for C_v and C_δ as functions of temperature for various frequencies, as described under MMA, heat capacity was calculated as a function of temperature. These values are summarised in Table-6 and plotted in Fig. (2). The following equation was then developed by the method of least squares :

$$C_p^\circ = -7{\cdot}73985 + 15{\cdot}9536 \times 10^{-2} T - 0{\cdot}877218 \times 10^{-4} T^2 + 0{\cdot}01814 \times 10^{-6} T^3 \quad (12)$$

44641

The C_p^o values calculated from this equation are plotted in Fig. (2) to indicate the accuracy of the proposed equation in the temperature range 300-1500°K. This equation holds good to within 2 per cent.

A C_p^o equation was also developed using the method of Rihani and Doraiswamy [8], as described under MMA, and the final equation is given below.

$$C_p^\circ = -10{\cdot}9246 + 18{\cdot}3193 \times 10^{-2} T - 1{\cdot}16100 \times 10^{-4} T^2 + 0{\cdot}02768 \times 10^{-6} T^3 \quad (13)$$

The values calculated by this procedure are also plotted in Fig. (2).

Heat of formation :

The heat of formation was calculated in the same manner as described under MMA. For estimating these values, ΔH_r° for the reaction

$$\text{ANILINE} + 2\,\text{METHANOL} \longrightarrow \text{DMA} + 2\,\text{WATER} \qquad \text{(ii)}$$

was first calculated. From the values of ΔH_r° and ΔH_f° of aniline, methanol and water at different temperatures, the ΔH_f° of DMA was calculated as a function of temperature. These values are listed in Table-6.

Free energy of formation :

Values of free energy of formation in the range

300-1500°K were calculated by van Krevelen's method[11]. The following two equations were developed for ΔG_f° as a function of temperature.

Range 300-600°K

$$\Delta G_f^\circ = 17{\cdot}484 + 12{\cdot}613 \times 10^{-2} T \qquad (14)$$

Range 600-1500°K

$$\Delta G_f^\circ = 12{\cdot}375 + 13{\cdot}348 \times 10^{-2} T \qquad (15)$$

A plot of ΔG_f° Vs T in the range 300-1500°K is shown in Fig. (4) and the values are summarised in Table-6.

Entropy :

The entropy change of the reaction was first calculated from Equation (10). Then, from a knowledge of ΔG_r° and ΔH_r°, the absolute entropy of DMA was estimated from the relationship,

$$\Delta S_r^\circ = S^\circ_{DMA} + 2S^\circ_{H_2O} - 2S^\circ_{MeOH} - S^\circ_{A} \qquad (16)$$

The estimated values are listed in Table-6.

log K_f :

log K_f values were estimated from Equation (3). The estimated values are summarised in Table-6.

Water

The reported thermodynamic properties of water[9] are tabulated in Table-3.

Heats of Reaction

The several possible reactions have been summarised at the beginning of this chapter. Heats of reaction for reactions (iv), (v), (vi) and (vii) were calculated from the ΔH_f° values of the products and reactants in the temperature range 298-1000°K. The final ΔH_r° equations were then developed by the method of least squares and are summarised in Table-7.

Heats of reaction for reactions (i), (ii) and (iii) were calculated as functions of temperature by using the general equation,

$$\frac{\Delta H_r^\circ}{T} = \frac{\Delta a}{1} + \frac{\Delta b}{2}T + \frac{\Delta c}{3}T^2 + \frac{\Delta d}{4}T^3 + \frac{I_H}{T} \qquad (17)$$

where Δa, Δb, Δc and Δd express the differences in the values of a, b, c and d between the products and reactants. The constants of integration (I_H) were determined from the reported values of ΔH_r° at 298°K. The final $\frac{\Delta H_r^\circ}{T}$ equations (298-1000°K) are summarised in Table-7.

The values of ΔH_r° for all the reactions in the temperature range 300-1000°K are tabulated in Table-8, and Figs. (5,6,7,8,9,10,11) show the plots of ΔH_r° Vs T.

Equilibrium constants

The equilibrium constants for all the reactions

were calculated from the equation,

$$\frac{\Delta G_r^\circ}{T} = -R \ln K \qquad (18)$$

where

$$\Delta G_r^\circ = \Delta G_f^\circ \text{ (products)} - \Delta G_f^\circ \text{ (reactants)} \cdots (19)$$

and the results are presented in Tables-9 and 10. Plots of log K vs $1/T$ for all the reactions appear in Figs. (12,13).

Equilibrium Conversions

The equilibrium conversions of the various reactions can be calculated from the general equation,

$$K = \left[\frac{n_R^r \times n_S^s}{n_B^b \times n_C^c} \right] \left[\frac{\Pi}{n_t} \right]^{\overline{r+s} - \overline{b+c}} K_\gamma \qquad (20)$$

where K_γ is the fugacity coefficient term. At ordinary pressure K_γ may be assumed to be unity over the entire temperature range. Using equation (20), a relationship of the form

$$K = f(x) \qquad (21)$$

was derived for each of the reactions. At any temperature, from a knowledge of K, Equation (21) was then solved by a trial and error procedure. This was repeated at several temperatures in the range 300-1500°K. Plots of the equilibrium conversion as a function of temperature for all the reactions appear in Figs. (14,15,16,17,18,19).

REFERENCE

1. Banerjee, S.C. and Doraiswamy, L.K., Brit. Chem. Eng. (In press).

2. Bennewitz, K. and Rossner, W.Z., Physik. Chem., 39B, 126 (1938).

3. Dobratz, C.J., Ind. Eng. Chem., 33, 759 (1941).

4. Evan, C.J., Spectrochim Acta, 16, 428 (1960).

5. Gordon, A.R., J. Chem. Phys., 2, 65 and 549 (1934).

6. Green, J.H.S., J. Appl. Chem., 11, 397 (1961).

7. Hatton, W.E., Hildenbrand, D.L., Sinke, G.C., and Stull, D.R., J. Chem. and Eng. Data, 7, No.2, 229 (1962).

8. Rihani, D.N. and Doraiswamy, L.K., Ind. Eng. Chem. (In press).

9. Rossini, F.D., Prosen, E.J.R. and Pitzer, K.S., J. Res., Natl. Bur. Standards, 27, 529 (1941).

10. Stull, D.R. and Mayfield, F.D., Ind. Eng. Chem. 35, 639 and 1303 (1943).

11. van Krevelen, D.W. and Chermin, H.A.G., Chem. Eng. Sci., 1, No.2, 66 (1951).

12. Vriens, G.M. and Hill, A.G., Ind. Eng. Chem. 44, 2732 (1952).

13. Hougen, O.A. and Watson, K.M.,"Chemical Process Principles Charts," (John Wiley and Sons, 1946), p166.

CHAPTER - 4

EXPERIMENTAL

Description of equipment

It was considered necessary to incorporate the following principal features in the experimental set-up: constant flow rates of aniline and methyl alcohol; constant vapourisation rates of the liquids; and isothermicity in the reaction zone. A diagrammatic sketch of the assembly is presented in Fig. (20) and a photograph of the assembly appears in Fig. (21).

Aniline and methyl alcohol were fed at constant rates from a D.C.L. duplex metering pump, which had provision for pumping two liquids simultaneously at any desired rate between 0 and 6 gallons per hour by adjustment of the graduated micrometer thimbles provided.

Methyl alcohol then entered a vapouriser, which consisted of a chamber heated by nicrome wire wound round the surface; a gauge glass indicated the level of the liquid in the chamber. Any desired feed rate, within the limits of the design, could be obtained by maintaining a constant level of the liquid by appropriate adjustment of the heat input. A similar vapouriser was provided for aniline. Details of both the vapourisers are shown diagrammatically in Fig. (22). The liquids, before entering the corresponding vapourisers, were introduced into drop counting adapters through appropriate nozzles, so that a constant check could be kept on the constancy

of the rates. In practice, for any liquid, the corresponding micrometer thimble of the pump was calibrated against the number of drops falling through the drop counting adapter, so that any desired rate could be maintained by counting the drops. Suitable cooler-condensers were provided between the vapourisers and the corresponding adapters to prevent the vapours from entering the adapters and interfering with the flow rates.

The vapours from the vapourisers then entered the reactor through a preheater, 30 mm dia. x 320 mm long, heated by electrical resistance wire, the heat input being controlled through a variac. The details of the reactor are shown in Fig. (23). It consisted essentially of a tube, 22 mm dia. x 295 mm long, with a catalyst support plate provided at a distance of 13 mm from the bottom. The top section of the reactor was provided with a thermowell to measure the temperature gradient in the reactor, and an outlet for the product vapours. The reactor was surrounded by a 60 mm dia. x 100 mm long steel block, which was wound by electrical resistance wire on its outer surface, the heat input being controlled through a variac. The steel block acted as a thermostat and ensured constancy of temperature to within 2°C. More elaborate methods of ensuring isothermicity were not found necessary as the main reaction involved was only slightly exothermic.

The products from the reactor were then collected

in a receiver through a condenser, and the uncondensed gases consisting mostly of dimethyl ether were not collected in the majority of runs. The liquid products were analysed by vapour phase chromatography as described under analysis.

Raw materials

Methyl alcohol :

Commercial methyl alcohol was treated for removing traces of water by refluxing with freshly burnt quick lime for 6 hours. It was distilled in an efficient fractionating column, and its water content was finally determined by Karl Fischer reagent.

Aniline :

Technical grade aniline was distilled first under atmospheric pressure and then under vacuum.

Operation

A known weight of catalyst (activated bauxite) was introduced into the reactor. The heating circuit was switched on till the required temperature was attained. The preheater was then heated to the desired temperature. The vapourisers were heated slowly so that there was no sudden pressure build-up in the preheater zone, thus eliminating any chance of the catalyst bumping out of the reactor.

As soon as steady conditions were attained in the

vapourisers, the two liquids were pumped at slow rates to avoid a sudden drop in temperature in the vapourisers. The rates were then gradually increased to the required levels. During a run several temperature traverses were taken to ensure constancy of temperature throughout the catalyst bed.

Although from thermodynamic calculations it was clear that the reaction was slightly exothermic, during a run no appreciable rise in temperature was noticed, and reactor heating was therefore continued throughout the run. Reaction products were collected periodically for analysis.

Product analysis

For analysis of mixtures of aniline, methylaniline and dimethylaniline, two broad methods are possible : chemical methods, and physical methods.

Chemical methods

These consist essentially of determining aniline and dimethylaniline in the mixture separately and then calculating the amount of methylaniline present.

Aniline can be determined by coupling the diazo solution of aniline with excess standard solution of R - salt, or by titrating with m-phenylenediamine in buffered acetic acid medium. In both the cases, excess of coupling reagent is determined by titrating back with standard benzene diazonium chloride solution[2].

Aniline can also be determined by using picryl chloride [4], the reaction involved being :

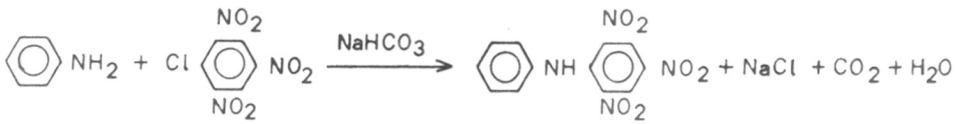

The sodium chloride formed can be estimated gravimetrically as silver chloride, or by titrating the solution potentiometrically with standard silver nitrate solution.

Dimethylaniline can be determined in the presence of aniline and methylaniline from the fact that acetic anhydride has negligible effect on dimethylaniline at low temperatures, while the other two are acetylated. This method therefore consists in titrating dimethylaniline, after acetylation of aniline and methylaniline at a low temperature, with perchloric acid in glacial acetic acid using α-naphthol benzein as indicator [1].

All the methods mentioned above were tried. The estimation of aniline by diazo and coupling titrations was not found to be very accurate, while the picryl chloride method was accurate but time consuming. The estimation of dimethylaniline by perchloric acid titration was tried by using indicators like cresol red, but was not found to be satisfactory as the end point was not very sharp. Due to these reasons attention was diverted to physical methods of analysing the mixture.

Separation by vapour phase chromatography (V.P.C.)

For the separation of aniline, methylaniline, and dimethylaniline by vapour phase chromatography, James and Martin[3] have suggested columns with paraffin wax, Lubrol MO (I.C.I.) and benzyl diphenyl as stationary phases and nitrogen as mobile phase.

During the present investigation, Perkin-Elmer Vapour Fractometer 154 D and Aerograph A-350-B models were used under the following conditions.

Perkin-Elmer Vapour Fractometer 154 D :		
Quantity of mixture introduced (for one injection)	=	4 µl
Column length	=	2 meters
Stationary phase	=	Apizone 'L' grease
Gas (mobile phase)	=	Hydrogen
Pressure of the gas	=	25 psi
Column temperature	=	150°C
Chart speed	=	1"/hr
Aerograph A-350-B :		
Quantity of mixture introduced (for one injection)	=	1·5 µl
Column length	=	5 feet
Stationary phase	=	Silicon
Gas (mobile phase)	=	Hydrogen
Flow rate of the gas	=	50 cc/min
Column temperature	=	160°C

Collector temperature	=	200°C
Detector temperature	=	200°C
Injector temperature	=	210°C
Chart speed	=	30"/hr

Sample analysis

The material from the water condenser consisted of aniline, methylaniline, dimethylaniline, water, methanol and methyl ether. This formed two separate layers, an oily layer containing dimethylaniline, methylaniline and aniline and an aqueous layer containing water, methanol and traces of methyl ether dissolved in water. The bulk of the dimethyl ether formed during this reaction was allowed to escape and was not measured.

The oily layer was separated, weighed, washed with brine solution to remove any methyl alcohol, and was finally dried over sodium sulphate. The mixture after drying was stored and analysed by V.P.C. as described above. By measuring the area of each peak, the relative amounts of aniline, methylaniline and dimethylaniline were found. Then, from a knowledge of the total weight of the mixture, the amount of each component by weight was determined.

Sample calculation :

Basis : 1 hour

Aniline fed	=	0.2032 gm. moles.
Methanol fed	=	1.066 gm. moles.

From V.P.C. results [Fig. (24)],

Dimethylaniline formed	=	0.0646 gm. moles.

Methylaniline formed = 0.1169 gm. moles.

Aniline unreacted = 0.0217 gm. moles.

Conversion to dimethylaniline = $\frac{0.0646}{0.2032}$ x 100

= 31.78%.

Conversion to methylaniline = $\frac{0.1169}{0.2032}$ x 100

= 57.53%.

Unconverted aniline = $\frac{0.0217}{0.2032}$ x 100

= 10.69%.

REFERENCES

1. Hanna, G.J. and Siggia, S., Analytical Chemistry 34, 547 (1962).

2. Haslan, J., Sweeney, F., The Analyst, 70, 413 (1945).

3. James, A.T., Martin, A.J.P., Anal. Chem., 28, 1564 (1956).

4. Linke, B., Preissecker, H., Stadler, J., Ber., 65, 1280 (1932).

CHAPTER - 5

RESULTS AND DISCUSSION

Homogenous reaction

In studying the kinetics of a vapour phase catalytic reaction, it is necessary to ascertain the extent of any homogenous reaction that may occur in the void spaces of the catalyst bed. The reaction occurring on the catalyst surface will then be the difference between the total reaction and that taking place in the void spaces.

Experiments were conducted at a temperature of 375^{o} using very low feed rates to evaluate the homogenous reaction. In all the runs carried out for this purpose (at different rates of flow), there was no observable conversion either to MMA or DMA. The rate data obtained by using a catalyst may therefore be directly used for the correlation of catalytic reaction rates.

Activation of bauxite

It is generally known that alumina is a very effective catalyst for this reaction. The use of bauxite and several other catalysts has also been reported in the literature, and these have been briefly discussed in Chapter II. In the present investigation it was decided to make a process study of the condensation of methyl alcohol and aniline using Indian bauxite as catalyst. The composition of the bauxite used is given below.

		%
Moisture and volatile matter	..	10.47
Silica	..	26.02
Alumina	..	61.42
Iron oxide	..	1.80
Titanium oxide	..	0.29

The use of bauxite for other dehydration reactions, such as dehydration of ethanol, requires an activation temperature of about 400° and activation time of about 4 hours. As a first step in the use of bauxite for the present reaction, the effect of using different activation temperatures and times was evaluated, and the results are summarised in Table-11. It can be seen from this table and Fig. (25) that activation at 400° for a period of 4-5 hours gives the most favourable result. In all the runs reported in this work, the catalyst was activated under these conditions.

Mass transfer effect

It is necessary to eliminate the resistance due to mass transfer before obtaining reaction rate data. If this is not done, the mass transfer resistance under the conditions used should be estimated from generalised procedures, and the actual reaction rates calculated from a knowledge of the experimental rates and the estimated mass transfer resistance. This procedure can be avoided by obtaining the experimental data at such velocities where the effect of mass transfer can be neglected. At these high velocities concentration gradients across the

film surrounding the catalyst particles may be neglected, and concentrations in the bulk stream may be taken as equal to those on the catalyst surface.

In organising the experimental work, therefore, two distinct effects have to be considered : (1) mass transfer effect; and (2) kinetic effect. In order to evaluate the mass transfer effect it is obvious that the kinetic effect should be maintained constant. This can be achieved by operating the reactor at different feed velocities but at the same value of W/F_1. This situation, requiring varying feed velocities but constancy of W/F_1, can be obtained by varying both W and F_1 such that W/F_1 remains constant.

Three series of runs were carried out at W = 8 gm, W = 12 gm and W = 16 gm, and for each series the feed rate was varied maintaining a constant ratio of methyl alcohol and aniline. The results are summarised in Table-12 and plotted in Fig. (26). Beyond W/F_1 = 70 the three curves tend to merge together, but below this value the effect of mass transfer evidently cannot be ignored.

A cross plot of Fig. (26) giving conversion as a function of feed velocity is shown in Fig. (27). For any given W/F_1 it was ensured that the feed velocity was maintained at a value higher than that required for the absence of mass transfer resistance at that W/F_1.

Life test

Before undertaking kinetic investigations on the

catalyst, life tests were carried out for the following principal reasons : (1) to ensure that all the kinetic data were taken with catalyst samples of equal and reproducible activity, and (2) to ascertain the catalyst life for making an economic assessment of the process.

A continuous run was carried out for a period of 100 hours and conversions were determined at several intervals during this period. The results plotted in Fig. (23), clearly show that the catalyst maintains a uniform activity for about 80 hours, after which there is a steep fall in the conversion.

Work on the reactivation of the catalyst may be desirable, but this does not form the part of the present investigation.

The data presented in subsequent sections were all obtained using bauxite samples drawn from the same bulk source, each sample being used for a period much less than the active life of the catalyst.

Effect of aniline-methanol ratio

From the stoichiometry of the reaction involved, it is clear that at a ratio of about 1:1 MMA should be the predominant product. As the present investigation was undertaken with the chief objective of determining the conditions for the production of DMA, several runs were organised at ratios greater than 1:1 and conversion to DMA determined at each of these ratios. The results,

summarised in Table-13 and presented graphically in Fig. (29), indicate a steep rise in the conversion to DMA when the ratio is increased from 1:2 to 1:4, after which there is a tendency to level off. A ratio of 1:5 was chosen for all the subsequent studies.

Product distribution

In a complex reaction of this type where several competing reactions occur simultaneously, it is difficult to quantitatively resolve the effects of individual reactions. As a first step in the correlation of data for such reactions, it is customary to prepare product distribution plots. These plots may be presented either as (1) overall conversion of a selected key component vs fraction of the key component going to each of several products, or as (2) conversion of a selected key component to each of several products as a function of W/F_1. Plot (2) gives a clearer representation of the reaction mechanism involved and is more helpful in the correlation of the data.

In the present study the following ranges of variables have been used in preparing product distribution plots :

(1) W/F_1 - 15 to 150

(2) Temperature - 300° to 400°

(3) Ratio of reactants - 1:2 to 1:5

(a ratio of 1:5 was maintained during the kinetic experiments)

The product distribution plots at 300°, 350°, and 375° appear in Figs. (30, 31 and 32). From these plots the following general observations may be made :

(1) The conversion to DMA increases with increase in W/F_1 and levels off at a particular value of W/F_1, this value decreasing with increase in temperature. As DMA is the final product in these reactions, this trend is according to expectations.

(2) The conversion to MMA increases with increase in W/F_1, reaching a maximum value, and then decreases. This trend is to be expected for any intermediate product in a complex reaction. The position of the maximum in these curves is determined by the relative rates of formation and disappearance of MMA. At a temperature of 300°, there is a considerable formation of MMA, and maximum conversion occurs at a W/F_1 of approximately 45, corresponding to a conversion of 62 per cent. At 350° the maximum conversion occurs at a W/F_1 of approximately 35, corresponding to a conversion of about 45 per cent. When the temperature is increased to 375°, the maximum conversion obtained is about 28 per cent at a W/F_1 of 20. It will thus be seen that the rate of disappearance of MMA increases with increase in temperature.

(3) The figures also show a plot of unreacted aniline as a function of W/F_1. It is evident that the overall rate of disappearance of aniline increases sharply with increase in temperature.

(4) Experiments were also conducted at 400°, but these are not plotted as the results did not conform to any pattern and were not reproducible. A few experiments were found to be reproducible, and these have been utilised in the correlation of data discussed in the next section.

Correlation of data

It is theoretically possible to attempt a rigorous correlation of the data presented in Figs. (30) through (32) by resolving the rates of the individual reactions, but in the present work pseudo-first-order kinetics in terms of a key reactant has been assumed, in this case aniline, and an appropriate design equation has been developed. The assumption of pseudo-first-order kinetics is justified as the second reactant involved is present in large excess.

The usual methods of determining first order equations were attempted but the resulting correlations were not satisfactory. It was therefore decided to correlate the data in two regions of conversion, low and high. Assuming pseudo-first-order kinetics and neglecting the reverse reaction, the following rate equation may be written :

$$r = k\,(1 - x) \qquad .. \qquad (1)$$

Then, from the relation,

$$W/F_1 = \int \frac{1}{r}\, dx \qquad .. \qquad (2)$$

the following equation can be developed :

$$W/F_1 = \frac{1}{k} \ln \left(\frac{1}{1 - x} \right) \quad .. \quad (3)$$

Equation (3) is best used for the low conversion - high space velocity region, since a plot of $\log \left(\frac{1}{1 - x} \right)$ vs W/F_1 must yield a straight line which extrapolates to $W/F_1 = 0$, thus rigidly fixing one point on the line.

For the high conversion - low space velocity region, on the other hand, Equation (3) can be re-written to give :

$$F_1/W = k \frac{1}{\ln \left(\frac{1}{1 - x} \right)} \quad .. \quad (4)$$

Thus a plot of $1 / \log \left(\frac{1}{1 - x} \right)$ vs F_1/W should now give a straight line which must extrapolate to $F_1/W = 0$.

As most of the points obtained were in the high conversion region, Equation (4) has been used, and a plot of this equation at 350°, 375° and 400° appears in Fig. (33). The values of the rate constant, k, were computed by measuring the slopes of these lines and are given below.

T	k
623	3.30×10^{-2}
648	9.8×10^{-2}
673	20.5×10^{-2}

The rate constants were then correlated with temperature as shown in Fig. (34), the corresponding equation being :

$$k = 4.093 \times 10^{8} e^{-1.441 \times 10^{4}/T} \quad .. \quad (5)$$

The final rate equation may therefore be written as :

$$r = 4.093 \times 10^{8} e^{-1.441 \times 10^{4}/T} (1-x) \quad .. \quad (6)$$

Low conversion values were available only at 300°, and these have been plotted according to Equation (3) in Fig. (35), but no correlation with respect to temperature has been attempted since low conversion data at other temperatures were not available. At 300° the rate equation is given by

$$r = 3.815 \times 10^{-2} (1-x) \quad .. \quad (7)$$

The correlations proposed have been verified by calculating k from Equation (5) and W/F_1 from Equation (4), and comparing the calculated values with those read from the curves of Figs. (30, 31 and 32). Fig. (36) shows a plot of experimental vs calculated values from which the average deviation has been estimated as 4.5 per cent.

Selectivity

The equations proposed so far are for the overall conversion of the key component (aniline). As we are interested in the conversion of aniline to DMA it is convenient to define a suitable selectivity term :

$$\text{Selectivity (s)} = \frac{\text{moles of DMA formed}}{\text{moles of aniline converted}} \qquad (8)$$

Plots of selectivity vs W/F_1 for the three temperatures appear in Fig. (37), from which it is immediately evident that the behaviour of selectivity is in general similar to that of overall conversion of aniline.

Fig. (38) shows a log-log plot of selectivity as a function of overall conversion. It may be seen that selectivity is higher at lower conversion of aniline, while at total conversion selectivity also approaches unity. An empirical correlation of the straight lines of Fig. (38) gives an equation of the form,

$$s = x^n \quad \text{(intercept = 1)} \qquad (9)$$

The index, n, depends upon the temperature of the reaction and can be correlated as shown in Fig. (39), the corresponding equation being :

$$n = 0.332\, e^{(1.62 \times 10^{-3})\, T} \qquad (10)$$

Equations (6, 7, 9 and 10) can be directly used for the design of a reactor for the production of DMA.

TABLES

Table-1

Thermodynamic Functions of Aniline in the Ideal Gaseous State (7)

T^{o}_{K}	C^{o}_{P} Cal./^{o}K./gm-mole	S^{o}_{T} Cal./^{o}K./gm-mole	$(H^{o}_{T} - H^{o}_{0})$ Cal./gm-mole	$-(G^{o}_{T} - H^{o}_{0})/T$ Cal./^{o}K./gm-mole
298.15	25.91	76.28	4,349	61.69
300	26.07	76.44	4,397	61.78
350	30.28	80.78	5,807	64.19
400	34.17	85.08	7,421	66.53
450	37.68	89.31	9,218	68.83
500	40.81	93.45	11,182	71.09
600	46.09	101.37	15,536	75.48
700	50.32	108.81	20,365	79.72
800	53.79	115.76	25,575	83.79
900	56.71	122.27	31,105	87.71
1000	59.18	128.37	36,903	91.47

Table-1 (Continued)

T°_{K}	ΔH°_{f} K-Cal./gm-mole	ΔG°_{f} K-Cal./gm-mole	log K_f
298.15	20.80	39.90	-29.246
300	20.78	40.01	-29.143
350	20.12	43.36	-27.075
400	19.54	46.64	-25.482
450	19.03	50.10	-24.331
500	18.59	53.53	-23.398
600	17.88	60.59	-22.070
700	17.34	67.76	-21.156
800	16.95	74.97	-20.480
900	16.69	82.28	-19.979
1000	16.55	89.55	-19.571

Table-2

Thermodynamic Functions of Methyl Alcohol in the Ideal Gaseous State (6)

T^{o}_{K}	C^{o}_{P} Cal./^{o}K./gm-mole	S^{o}_{T} Cal./^{o}K./gm-mole	$(H^{O}_{T} - H^{O}_{O})$ K-Cal./gm-mole	$-(G^{O}_{T} - H^{O}_{O})/T$ Cal./^{o}K./gm-mole
273.16	10.15	56.39	2.473	47.33
298.16	10.49	57.29	2.731	48.13
300	10.52	57.36	2.751	48.19
400	12.29	60.61	3.887	50.90
500	14.22	63.56	5.213	53.14
600	16.02	66.32	6.727	55.11
700	17.62	68.91	8.411	56.90
800	19.04	71.36	10.245	58.55
900	20.29	73.67	12.210	60.11
1000	21.38	75.87	14.300	61.58

Table-2 (Continued)

T°_K	$-\Delta H^{\circ}_f$ K-Cal./gm-mole	$-\Delta G^{\circ}_f$ K-Cal./gm-mole (reported)	log K_f	$-\Delta G^{\circ}_f$ K-Cal./gm-mole (calculated)
273.16	47.72	39.46	31.56	-
298.16	47.94	38.70	28.36	38.6630
300	47.96	38.64	28.14	-
400	48.81	35.41	19.34	35.3704
500	49.57	31.97	13.97	31.9283
600	50.11	28.38	10.34	28.3500
700	50.74	24.70	7.71	-
800	51.18	20.96	5.72	20.9144
900	51.53	17.16	4.17	-
1000	51.79	13.32	2.91	13.1845

Table-3

Thermodynamic Functions of Water in the Ideal Gaseous State (9)

T^{o}_{K}	C^{o}_{P} Cal./^{o}K./gm-mole	S^{o}_{T} Cal./^{o}K./gm-mole	$(H^{o}_{T} - H^{o}_{0})$ K-Cal./gm-mole	$-(G^{o}_{T} - H^{o}_{0})/T$ Cal./^{o}K./gm-mole
298.16	8.028	45.109	2.365	37.175
300	8.030	45.159	2.379	37.224
400	8.190	47.789	3.190	39.512
500	8.421	49.340	4.019	41.299
600	8.685	50.898	4.873	42.773
700	8.968	55.258	5.755	44.032
800	9.264	53.475	6.666	45.137
900	9.570	54.583	7.606	46.127
1000	9.881	55.609	8.580	47.023

Table-3 (Continued)

T°_K	$-\Delta H^{\circ}_f$ K-Cal./gm-mole	$-\Delta G^{\circ}_f$ K-Cal./gm-mole	log K_f
298.16	57.794	54.638	40.050
300	57.803	54.618	39.790
400	58.042	53.521	29.242
500	58.276	52.363	22.380
600	58.500	51.160	18.638
700	58.707	49.918	15.585
800	58.900	48.648	13.290
900	59.077	47.357	11.500
1000	59.234	46.046	10.063

Table-4

Thermodynamic Functions of Methyl Ether in the Ideal Gaseous State[1]

T°_K	C°_P Cal./°K./gm-mole	S°_T Cal./°K./gm-mole	$(H^{\circ}_T - H^{\circ}_0)$ K-Cal./gm-mole	$-(G^{\circ}_T - H^{\circ}_0)/T$ Cal./°K./gm-mole
300	15.890	63.848	3.447	52.355
400	20.820	69.151	5.313	55.876
500	22.087	73.370	7.256	58.858
600	23.189	77.746	9.625	61.688
700	27.897	82.180	12.340	64.551
800	29.886	85.640	15.190	66.665
900	32.194	89.182	18.180	68.996
1000	33.840	92.931	21.580	71.351

Table-4 (Continued)

T°_{K}	$-\Delta H^{\circ}_{f}$ K-Cal./gm-mole	ΔG°_{f} K-Cal./gm-mole	log K_f
300	43.323	26.1966	19.0826
400	45.390	20.2840	10.5076
500	45.545	15.0620	6.5830
600	47.405	7.7268	2.8142
700	48.036	1.4080	0.4396
800	48.622	-5.4100	-1.4778
900	49.160	-12.6410	-3.0690
1000	49.324	-18.6155	-4.0680

Table-5

Thermodynamic Functions of Monomethylaniline in the Ideal Gaseous State

$T^{\circ}K$	C_P° Cal./$^{\circ}K$/gm-mole	S_T° Cal./$^{\circ}K$/gm-mole	ΔH_f° K-Cal./gm-mole	ΔG_f° K-Cal./gm-mole	log K_f
300	28.330	72.061	20.528	50.697	-37.05
400	37.330	83.636	18.622	60.307	-31.40
500	45.620	95.140	17.005	69.897	-30.60
600	49.756	106.239	15.764	79.507	-28.60
700	59.120	114.884	14.544	88.935	-27.80
800	62.882	124.435	13.670	99.045	-27.05
900	66.865	132.691	13.105	109.145	-26.45
1000	70.215	140.609	12.950	119.255	-26.08
1100	73.195	-	-	129.409	-25.70
1200	75.675	-	-	139.523	-25.40
1300	77.764	-	-	149.637	-25.08
1400	79.664	-	-	159.751	-24.92
1500	81.185	-	-	169.865	-24.70

Table-6

Thermodynamic Functions of Dimethylaniline in the Ideal Gaseous State

T°_K	C°_p Cal./°K/gm-mole	S°_T Cal./°K/gm-mole	ΔH°_f K-Cal./gm-mole	ΔG°_f K-Cal./gm-mole	log K_f
300	32.748	88.222	20.366	55.314	-40.40
400	43.253	97.390	18.033	67.924	-35.50
500	53.038	108.955	16.062	80.534	-35.20
600	59.478	120.634	14.704	92.814	-33.90
700	67.833	124.629	13.206	105.835	-33.19
800	73.428	140.051	12.356	119.175	-32.55
900	78.143	149.222	11.795	132.475	-32.00
1000	82.118	158.072	11.733	145.975	-31.90
1100	85.658	-	-	158.903	-31.50
1200	88.618	-	-	172.551	-31.38
1300	91.118	-	-	185.899	-31.20
1400	93.368	-	-	199.247	-31.10
1500	95.208	-	-	212.595	-31.00

Table-7

Equations for Heats of Reaction in the Temperature range of 300° to 1000°K

S.No.	Reaction	$\frac{\Delta H_r^\circ}{T}$ =
(1)	A + MeOH → MMA + W	$-0.8271 + 0.744\times10^{-2}T - 0.186\times10^{-4}T^2 + 0.0110\times10^{-6}\times T^3 + \frac{10,104}{T}$
(2)	MMA + MeOH → DMA + W	$-3.4362 + 1.191\times10^{-2}T - 0.113\times10^{-4}T^2 + 0.0036\times10^{-6}T^3 - \frac{9,760}{T}$
(3)	A + 2MeOH → DMA + 2W	$-4.2634 + 1.945\times10^{-2}T - 0.297\times10^{-4}T^2 + 0.0147\times10^{-6}T^3 - \frac{19,888}{T}$
(4)	2MeOH → ME + 2W	$-0.0195 - 0.0017\times10^{-2}T + 0.00102\times10^{-4}T^2 - 0.00007\times10^{-6}T^3$
(5)	2A + ME → 2MMA + W	$-0.1274 + 0.0383\times10^{-2}T - 0.00480\times10^{-4}T^2 + 0.00021\times10^{-6}T^3$
(6)	2MMA + ME → 2DMA + W	$-0.1292 + 0.0388\times10^{-2}T - 0.00468\times10^{-4}T^2 + 0.00019\times10^{-6}T^3$
(7)	A + ME → DMA + W	$-0.1272 + 0.0386\times10^{-2}T - 0.00473\times10^{-4}T^2 + 0.00020\times10^{-6}T^3$

Table-8

Heats of Reaction (Values)

Reaction	Temp °K. →	$-\Delta H_r^\circ$ K-Cal./gm-mole			
		300	400	500	600
A + MeOH → MMA + W		10.095	10.150	10.291	10.506
MMA + MeOH → DMA + W		10.000	9.844	9.650	9.459
A + 2MeOH → DMA + 2W		20.100	19.971	19.939	19.956
2MeOH → ME + W		5.206	5.812	5.681	5.685
ME + 2A → 2MMA + W		14.986	14.488	14.901	15.327
2MMA + ME → 2DMA + W		14.804	13.830	13.617	13.214
A + ME → DMA + W		14.894	14.159	14.259	14.271

Table-8 (Continued)

Reaction	$-\Delta H_r^\circ$ K-Cal./gm-mole			
Temp °K. →	700	800	900	1000
A + MeOH → MMA + W	10.763	11.001	11.132	11.0438
MMA + MeOH → DMA + W	9.257	9.082	8.905	8.743
A + 2MeOH → DMA + 2W	20.068	20.034	19.989	19.706
2MeOH → ME + W	5.263	5.456	5.177	4.978
ME + 2A → 2MMA + W	16.263	16.838	17.087	17.110
2MMA + ME → 2DMA + W	13.347	12.906	12.537	12.347
A + ME → DMA + W	14.805	14.892	14.812	14.727

Table-9

Free Energy Changes of the Reactions

Reaction	Temp. °K. →	$-\Delta G_r^\circ$ K-Cal./gm-mole						
		300	400	500	600	700	800	900
A + MeOH → MMA + W		5.121	4.444	4.026	4.204	4.043	3.613	3.332
MMA + MeOH → DMA + W		11.461	10.494	9.756	9.132	8.298	7.558	6.867
A + 2MeOH → DMA + 2W		16.312	14.598	13.462	12.996	12.021	10.851	9.889
2MeOH → ME + W		39.520	38.982	38.485	38.091	37.895	37.308	36.959
A + ½ME → MMA + ½W		3.524	2.952	2.284	3.141	3.080	2.954	3.184
MMA + ½ME → DMA + ½W		9.594	9.001	8.014	8.294	7.355	6.899	6.619
A + ME → DMA + W		13.118	11.952	10.297	11.209	10.435	9.853	9.803

Table-9 (continued)

Reaction	Temp. °K. →	$-\Delta G_r^\circ$ K-Cal./gm-mole					
		1000	1100	1200	1300	1400	1500
A + MeOH → MMA + W		3.021	1.881	1.707	1.300	1.332	-0.134
MMA + MeOH → DMA + W		6.006	5.146	4.302	3.375	3.087	2.101
A + 2MeOH → DMA + 2W		8.385	9.027	7.410	4.675	4.419	1.967
2MeOH → ME + W		36.761	35.750	35.70	35.700	34.910	34.33
A + ½ME → DMA + ½W		2.622	2.096	2.212	1.422	1.205	0.558
MMA + ½ME → DMA + ½W		5.614	5.361	4.407	3.497	2.959	2.793
A + ME → DMA + W		8.236	7.457	6.619	4.918	4.164	3.351

Table-10

Reaction Equilibrium Constants

Reaction	Temp. °K. → 300	400	500	600	700	800	900
A + MeOH → MMA + W	5.383×10^{3}	2.679×10^{2}	7.031×10^{1}	3.396×10^{1}	1.821×10^{1}	9.654	6.443
MMA + MeOH → DMA + W	3.491×10^{8}	7.311×10^{5}	2.307×10^{4}	2.529×10^{3}	4.977×10^{2}	1.297×10^{2}	5.082×10^{1}
A + 2MeOH → DMA + 2W	77.62×10^{10}	93.97×10^{6}	76.21×10^{4}	53.95×10^{3}	56.62×10^{2}	91.83×10^{1}	25.23×10^{1}
2MeOH → ME + W	9.120×10^{28}	1.95×10^{21}	6.607×10^{16}	7.413×10^{13}	6.761×10^{11}	1.549×10^{10}	9.419×10^{8}
½ME + A → MMA + ½W	3.685×10^{2}	4.116×10^{1}	9.954	1.358×10^{1}	9.152	6.412	5.929
MMA + A → DMA + ½W	9.716×10^{6}	8.231×10^{4}	3.350×10^{3}	8.913×10^{2}	2.006×10^{2}	7.656×16^{1}	4.055×10^{1}
ME + A → DMA + W	3.581×10^{9}	3.388×10^{6}	3.334×10^{4}	1.211×10^{4}	1.937×10^{3}	4.909×10^{2}	2.404×10^{2}

Table-10 (continued)

Reaction	Temp. °K. → 1000	1100	1200	1300	1400	1500
A + MeOH → MMA + W	4.613	2.364	2.418	1.654	1.614	0.100
MMA + MeOH → DMA + W	2.208×10^{1}	1.112×10^{1}	6.334	3.806	3.113	2.058
A + 2MeOH → DMA + 2W	37.30	68.39	23.99	6.398	5.079	1.964
2MeOH → ME + W	1.081×10^{8}	1.259×10^{7}	3.162×10^{6}	1.000×10^{6}	2.818×10^{5}	1.000×10^{5}
$\frac{1}{2}$ME + A → MMA + $\frac{1}{2}$W	3.741	2.608	2.528	1.734	1.542	1.207
MMA + A → DMA + $\frac{1}{2}$W	1.687×10^{1}	1.161×10^{1}	6.342	3.870	2.897	2.549
ME + A → DMA + W	6.310×10^{1}	3.027×10^{1}	1.603×10^{1}	6.709	4.467	3.077

Table-11

Effect of Bauxite Activation Time and Temperature

W/F_1 = 55.25 gm-mole/hr./gm.

Run. No.	Activation Temp. °C.	Activation time hr.	Reaction Temp. °C.	$\frac{F_2}{F_1}$	Conversion to DMA %
1	400	1	375	5	81.25
2	400	2	375	5	92.80
3	400	4	375	5	95.26
4	400	6	375	5	95.92
5	400	4	340	3	35.38
6	460	4	340	3	35.00
7	600	4	340	3	35.90

Table-12

Effect of Mass Transfer

$F_2/F_1 = 3.65$

Run No.	Temp. °C.	W	F_1	W/F_1	Conversion to DMA %
1	375	8	0.10880	73.60	81.65
2	375	8	0.14507	55.20	77.46
3	375	8	0.29019	27.60	58.19
4	375	8	0.43520	18.40	60.00
5	375	12	0.12760	94.10	79.410
6	375	12	0.14507	82.75	83.58
7	375	12	0.43520	28.65	71.29
8	375	12	0.87044	13.80	56.67
9	375	16	0.12760	125.50	81.47
10	375	16	0.43520	36.78	77.00
11	375	16	0.65280	24.56	71.68
12	375	16	0.87044	18.30	65.46

Table-13

Effect of Methanol - Aniline Ratio on Product Distribution

Run No.	Temp. °C.	W/F_1	F_2/F_1	Product distribution as % aniline fed		
				Aniline	MMA	DMA
1	375	55.25	5	1.1	4.0	94.90
2	375	55.25	4	4.4	4.1	91.50
3	375	55.25	3.65	16	-	84.01
4	375	55.25	2	83.6	5.4	11.00
5	375	55.25	1	91	6	3.00

Table-14

Results of Kinetic Runs

$F_2/F_1 = 5$

Run No.	Temp. °C.	W	W/F_1	Product distribution as % aniline fed			DMA selectivity, %
				Aniline	MMA	DMA	
1	2	3	4	5	6	7	8
1	375	16	150.1	-	4.75	95.25	96.25
2	375	16	75.04	-	6.60	93.40	93.40
3	375	16	50.00	-	4.74	95.26	95.40
4	375	16	37.52	3.70	8.35	87.95	91.25
5	375	16	25.00	6.15	18.45	75.40	80.30
6	375	16	18.76	10.54	29.33	60.13	67.20
7	350	16	150.09	2.80	8.83	88.37	90.50
8	350	16	100.06	6.25	11.75	82.00	87.40
9	350	16	75.04	13.38	22.15	64.47	74.40
10	350	16	60.03	13.10	28.66	58.24	68.10

Contd.

Table-14 (continued)

1	2	3	4	5	6	7	8
11	350	16	50.00	19.35	35.65	45.00	55.75
12	350	16	37.52	15.50	46.30	37.70	44.69
13	350	16	25.00	28.48	36.82	34.70	48.55
14	350	16	20.13	37.90	33.90	28.20	45.35
15	300	12	78.25	9.32	49.18	41.50	45.80
16	300	12	59.06	10.68	57.52	31.80	35.80
17	300	12	46.51	16.059	63.29	20.66	20.20
18	300	12	37.51	22.90	59.18	17.92	23.25
19	300	12	29.53	34.39	52.41	13.20	20.20

Table of Symbols

A	-	aniline
C_p^o	-	heat capacity, cal./°K./gm-mole
DMA	-	dimethylaniline
F	-	total feed rate, gm-mole/hr.
F_1	-	aniline rate, gm-mole/hr.
F_2	-	methanol rate, gm-mole/hr.
ΔG_f^o	-	free energy of formation, K-cal./gm-mole
ΔG_r^o	-	free energy of reaction, K-cal./gm-mole
$\frac{G_T^o - H_O^o}{T}$	-	free energy function, cal./°K./gm-mole
ΔH_f^o	-	heat of formation, K-cal./gm-mole
ΔH_r^o	-	heat of reaction, K-cal./gm-mole
$H_T^o - H_O^o$	-	enthalpy function, K-cal./gm-mole
K	-	equilibrium constant
K_v	-	fugacity coefficient term
k	-	rate constant
MMA	-	monomethylaniline
ME	-	methyl ether
MeOH	-	methanol
n	-	number of moles
R	-	gas constant
r	-	reaction rate, gm-mole/hr./gm-cat.
s	-	selectivity
S_T^o	-	entropy, cal./°K./gm-mole
ΔS_r^o	-	entropy change of reaction, cal./°K./gm-mole
T	-	temperature, °K.

V.P.C.	-	vapour phase chromatography
W	-	wt. of catalyst, gm. (also water)
W/F	-	time function
x	-	overall conversion of anilines (also equilibrium conversion)
Π	-	total pressure, atm.

Subscripts of Superscripts

B,C, R & S	-	components in the general Equation (20)
b,c, r & s	-	stoichiometric proportions of B,C, R & S in Equation (20)

FIGURES

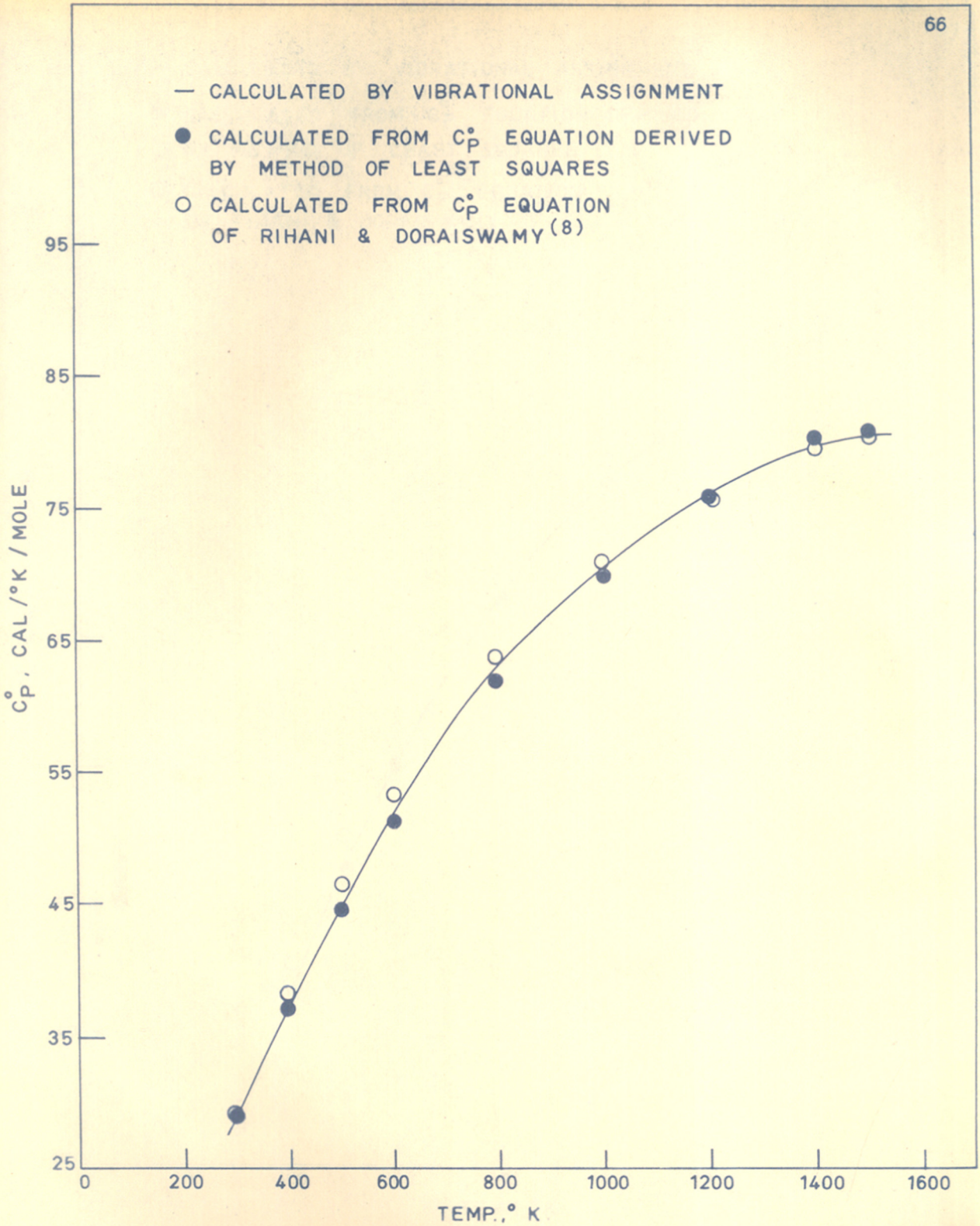

TEMPERATURE DEPENDENCE OF HEAT CAPACITY FOR MONOMETHYLANILINE

FIG. - 1.

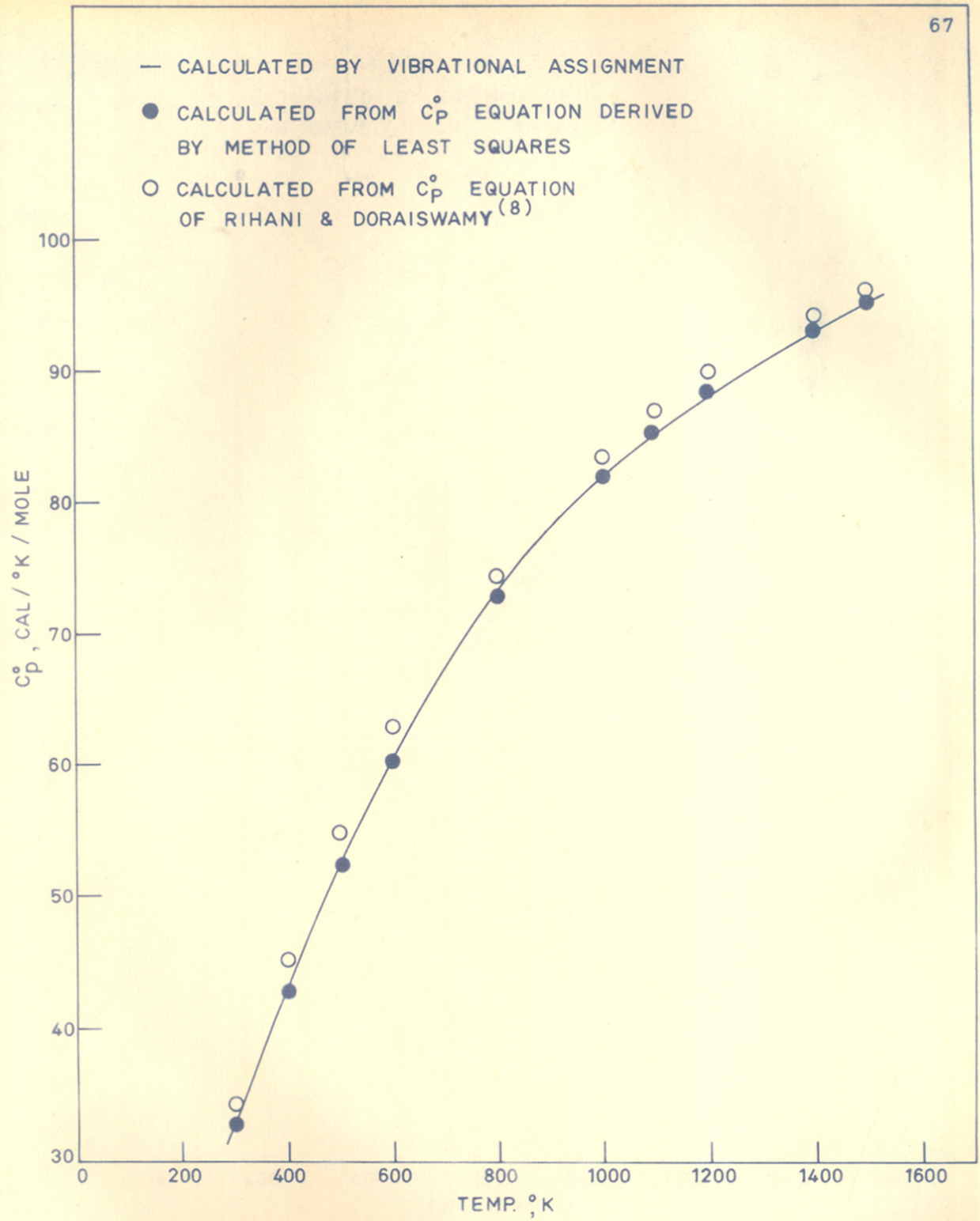

TEMPERATURE DEPENDENCE OF HEAT CAPACITY FOR DIMETHYLANILINE

FIG.– 2.

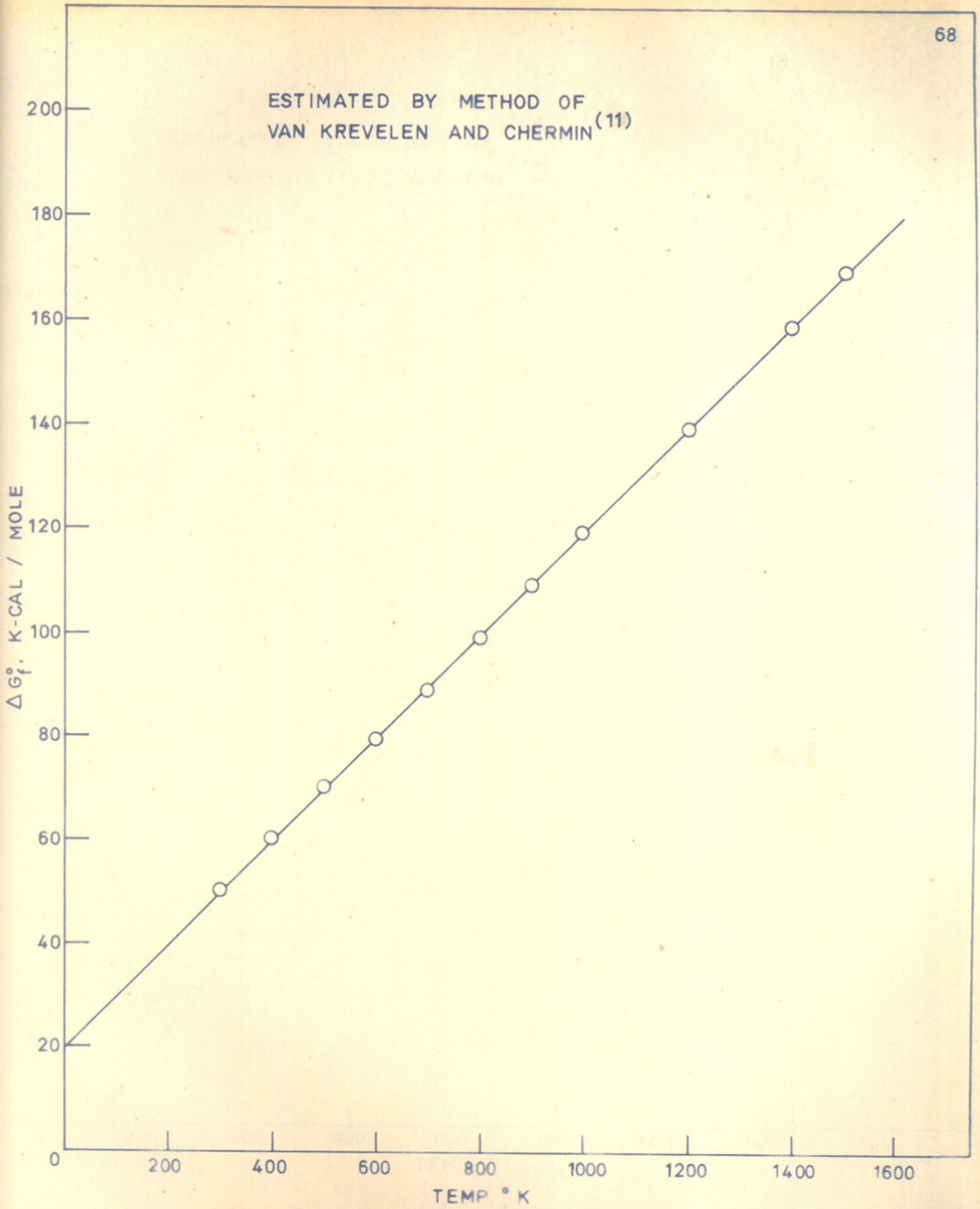

FREE ENERGY OF FORMATION OF MONOMETHYLANILINE AS A FUNCTION OF TEMPERATURE

FIG.-3.

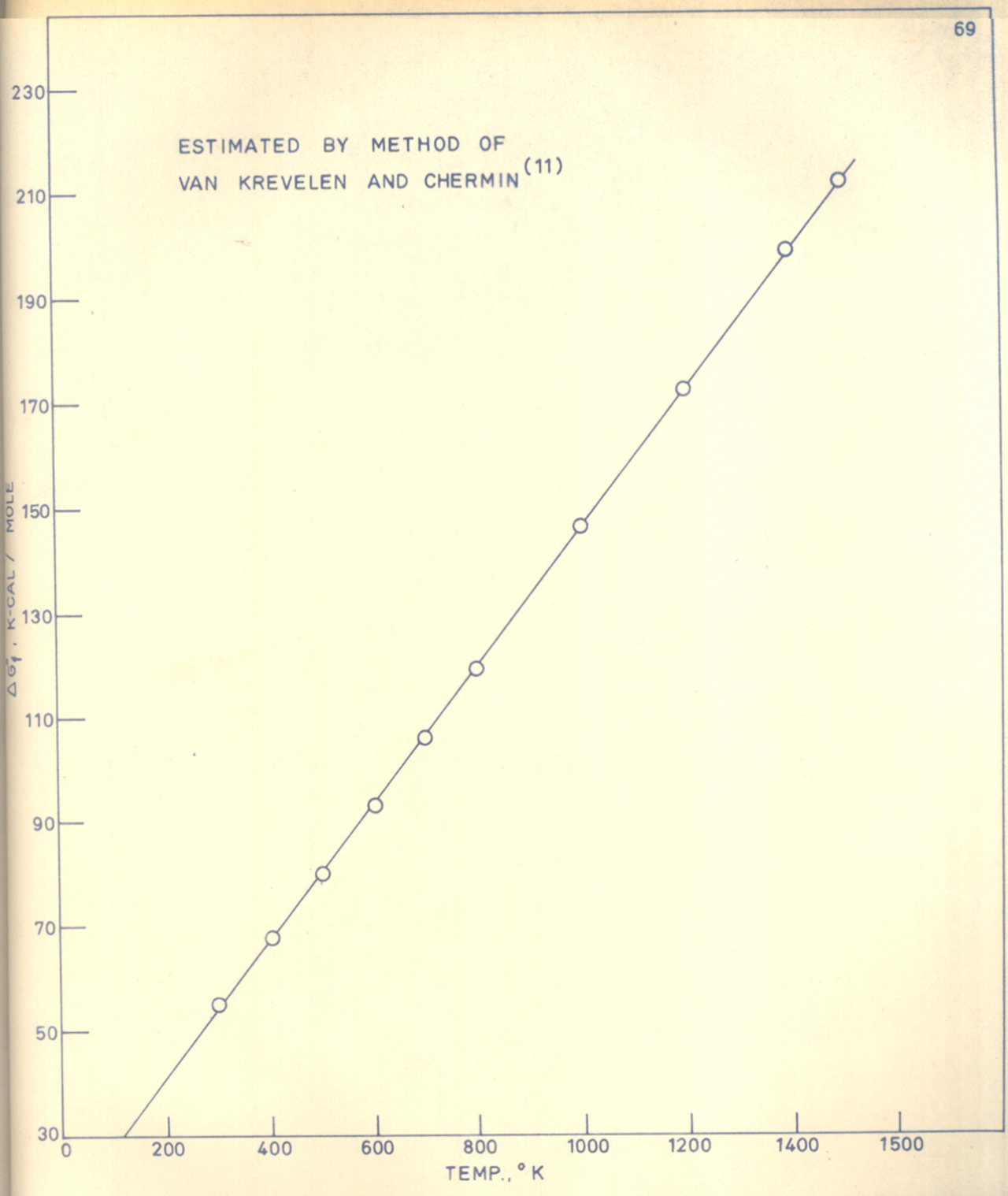

FREE ENERGY OF FORMATION OF DIMETHYLANILINE AS A FUNCTION OF TEMPERATURE

FIG.-4

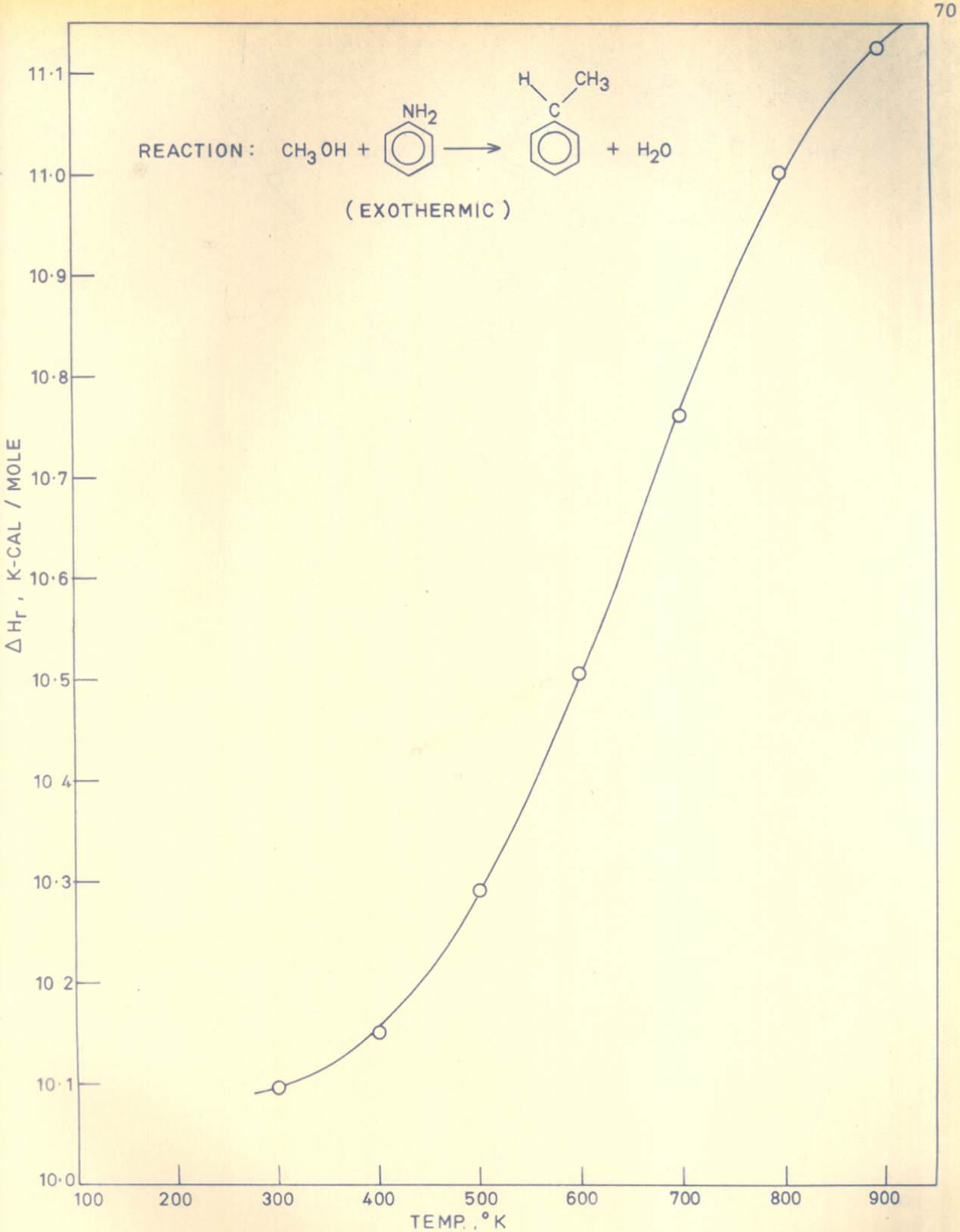

HEAT OF REACTION AS A FUNCTION OF TEMPERATURE FOR REACTION (1)

FIG.-5.

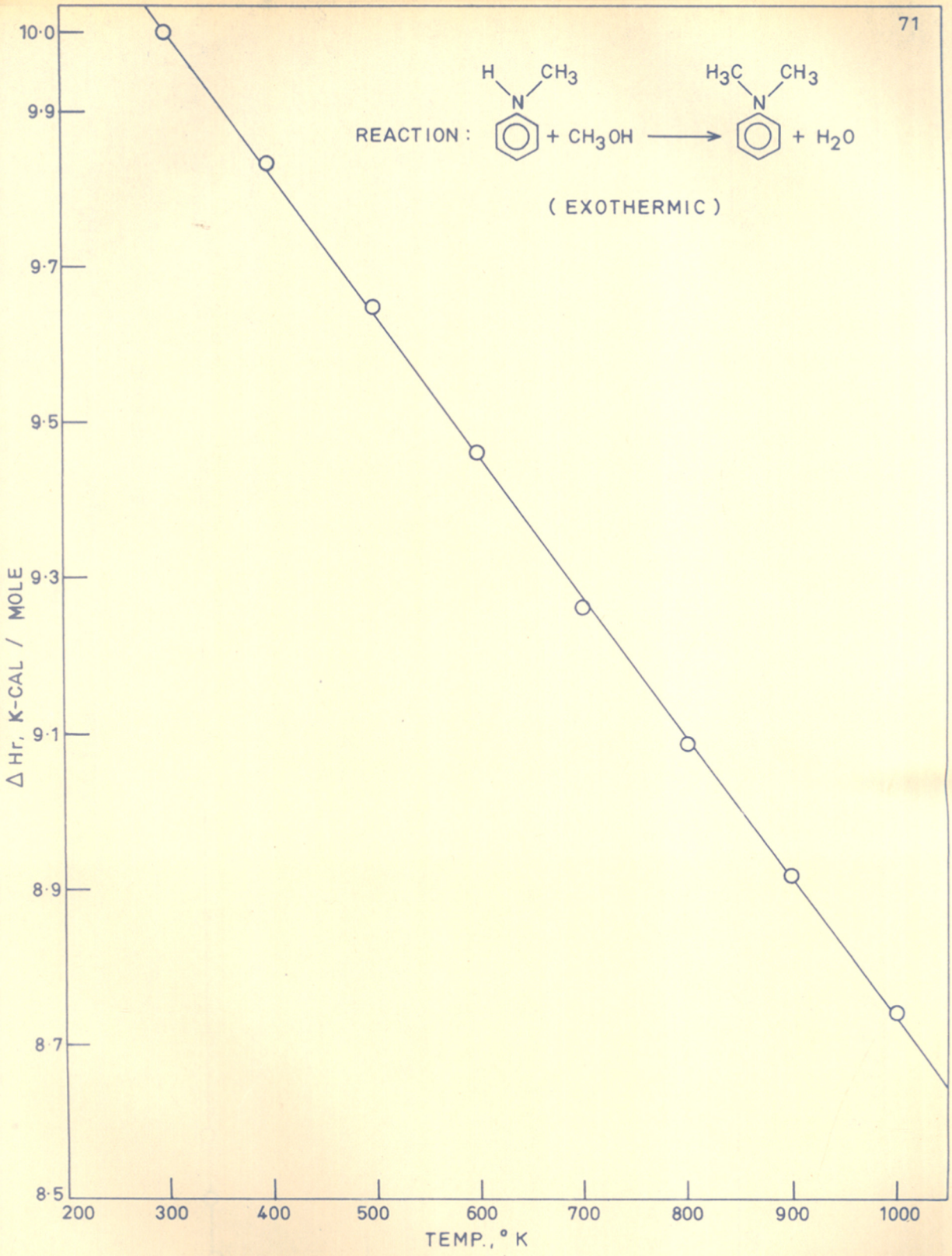

HEAT OF REACTION AS A FUNCTION OF TEMPERATURE FOR REACTION (II)

FIG.-6.

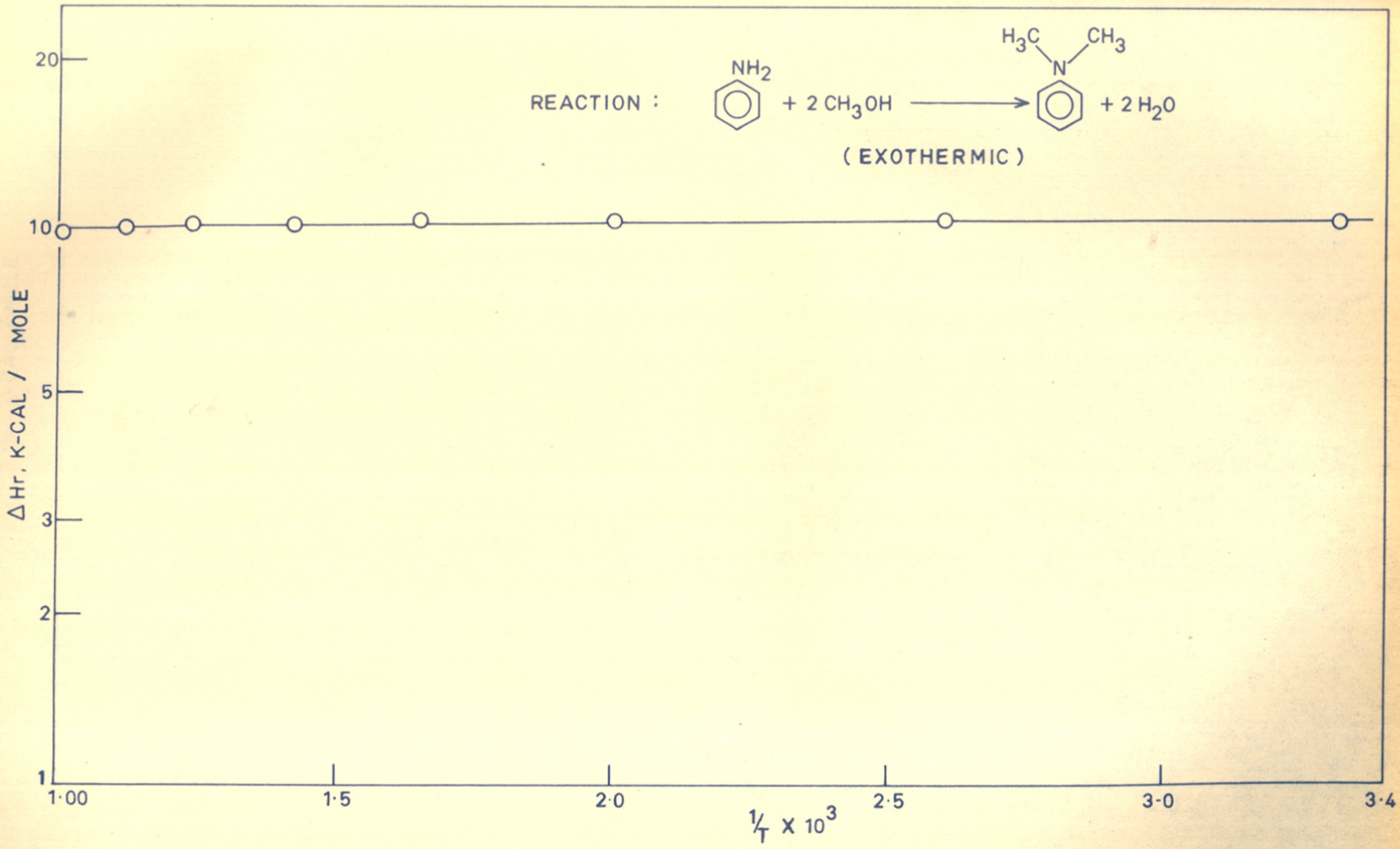

HEAT OF REACTION AS A FUNCTION OF TEMPERATURE FOR REACTION (III)

FIG. - 7.

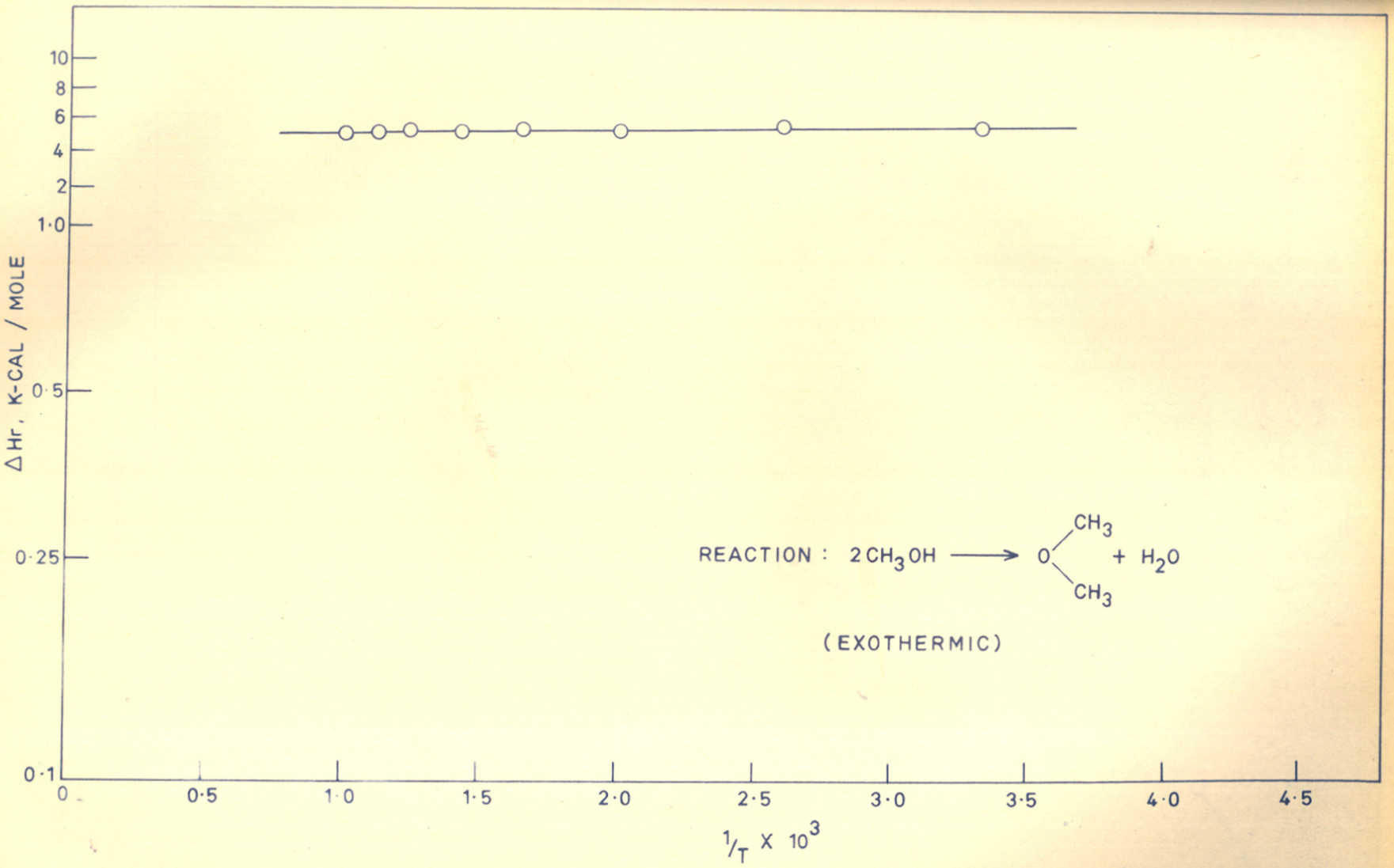

HEAT OF REACTION AS A FUNCTION OF TEMPERATURE FOR REACTION (IV)

FIG. - 8.

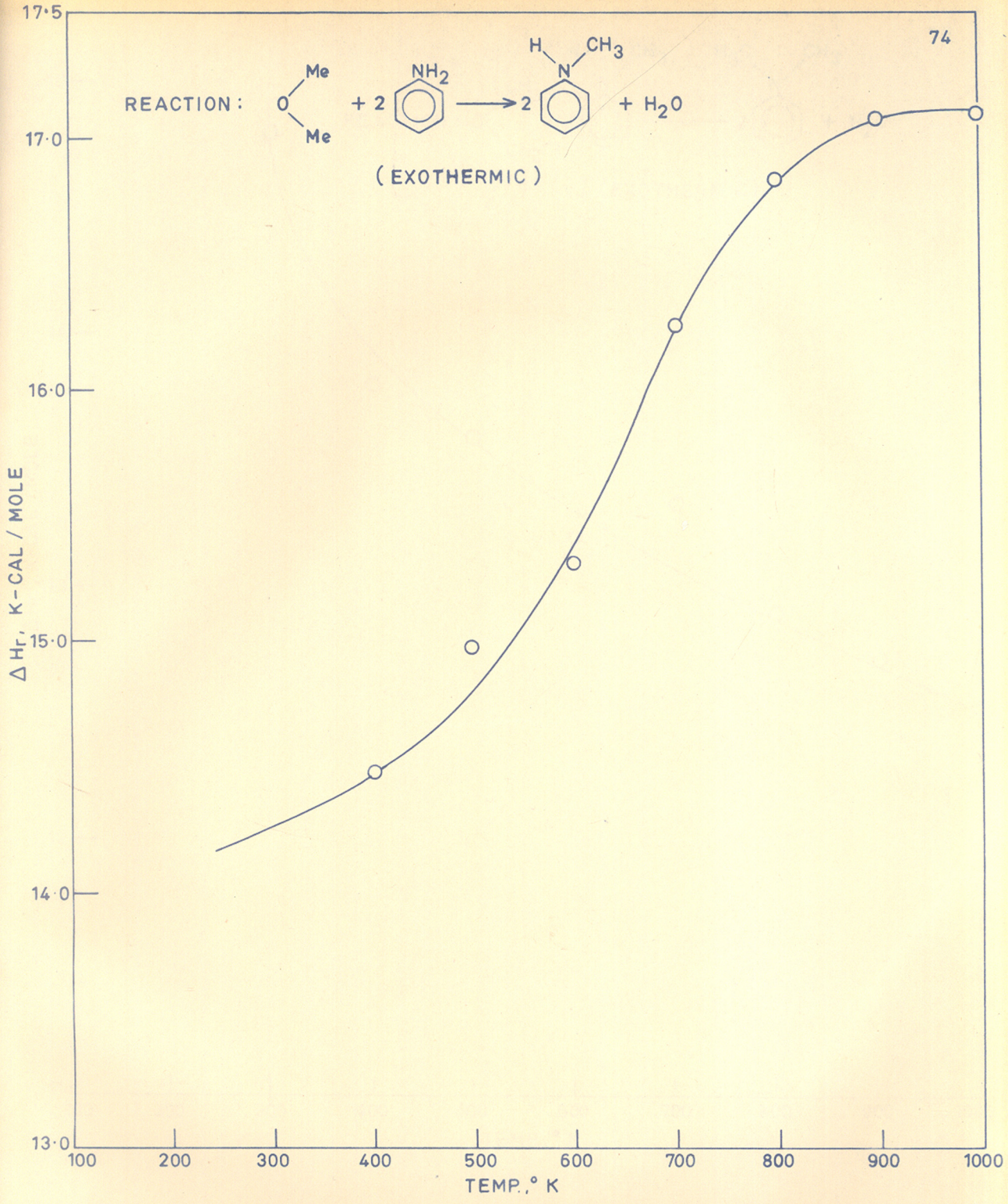

HEAT OF REACTION AS A FUNCTION OF TEMPERATURE FOR REACTION (V)

FIG. - 9

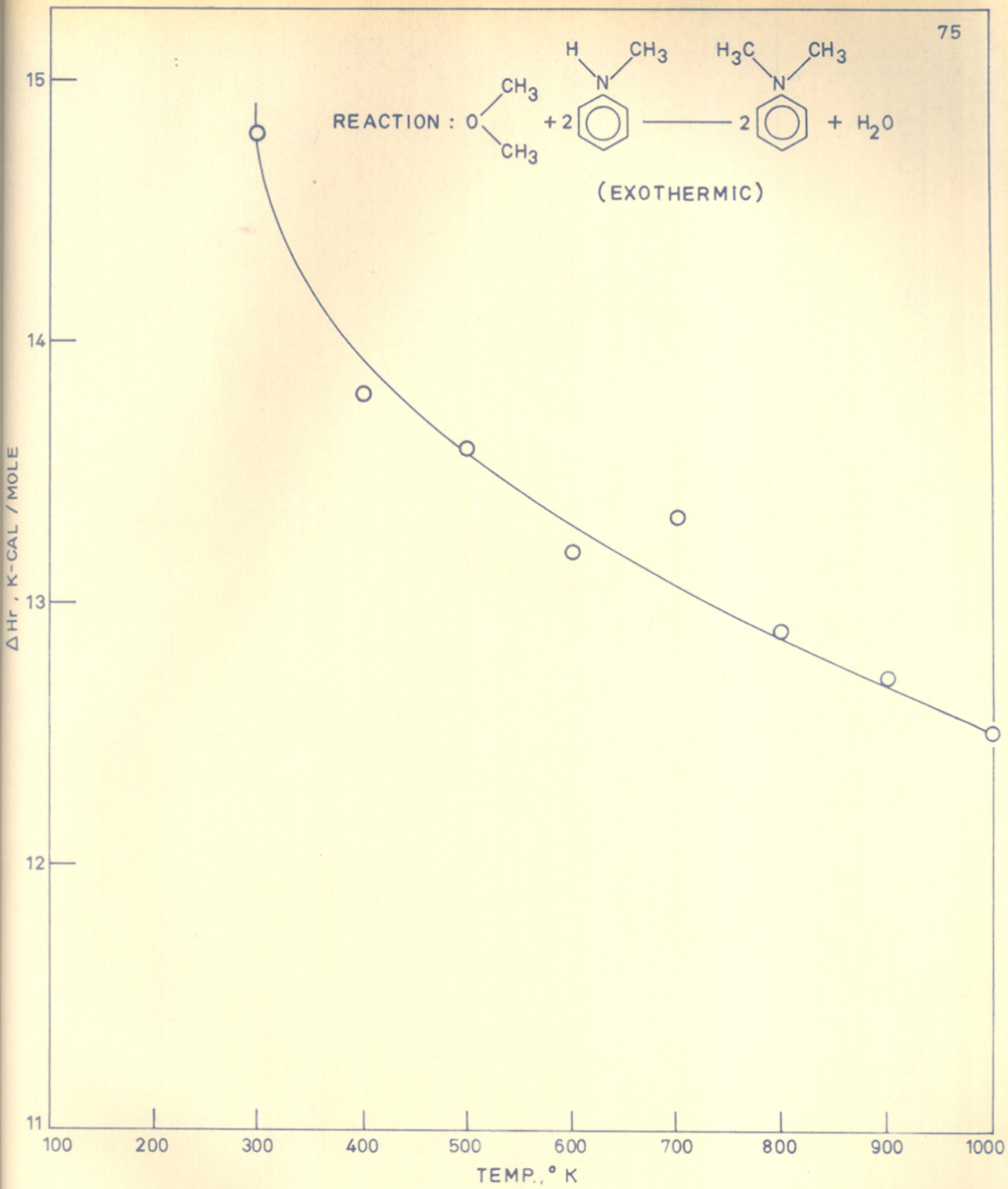

HEAT OF REACTION AS A FUNCTION OF TEMPERATURE FOR REACTION (VI)

FIG.-10.

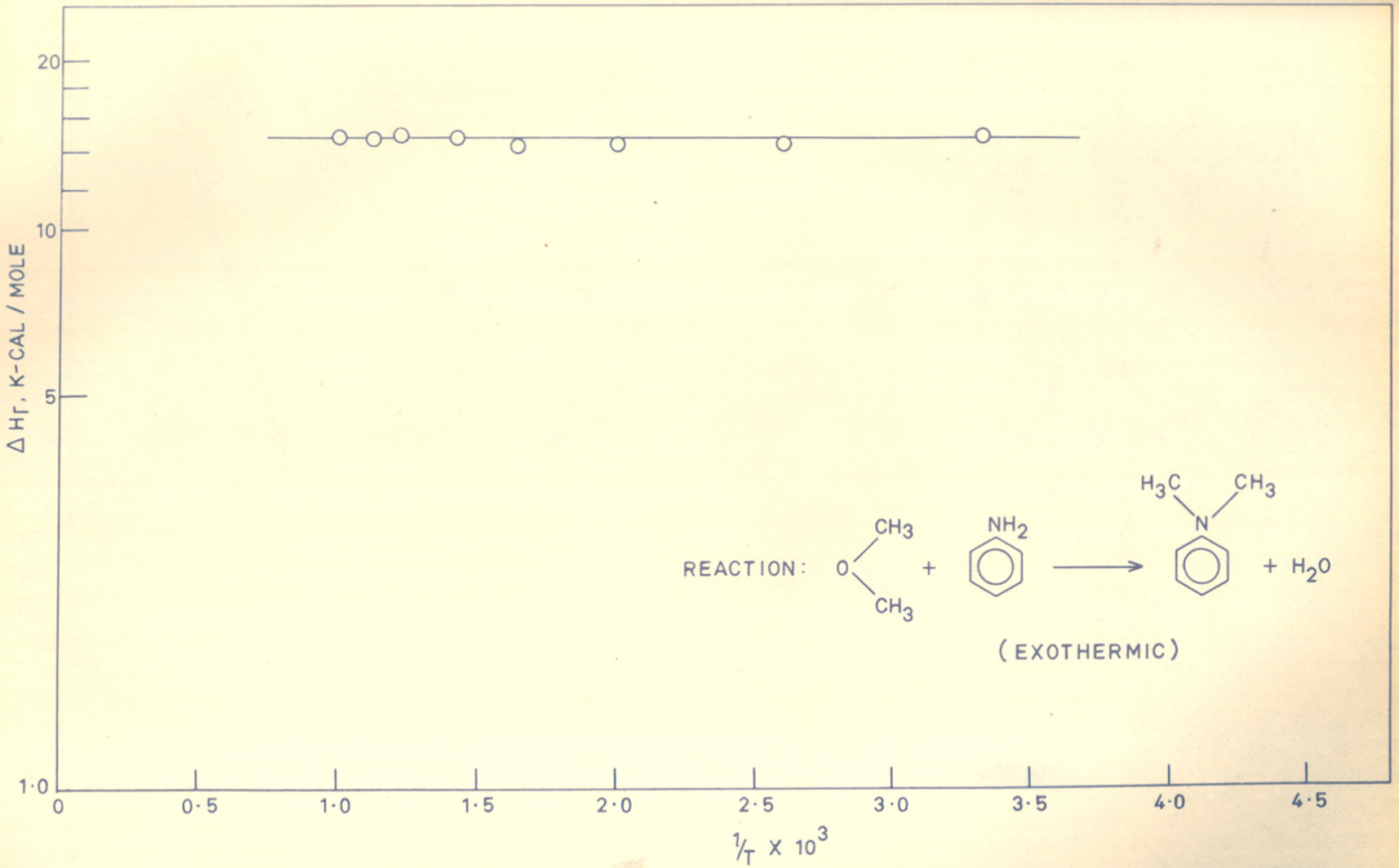

HEAT OF REACTION AS A FUNCTION OF TEMPERATURE FOR REACTION (VII)

FIG.-11.

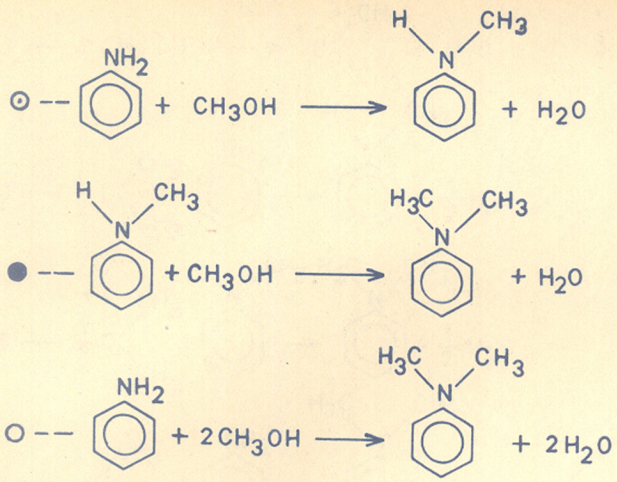

LOG K – 1/T PLOTS FOR REACTIONS (I, II & III)

FIG. – 12.

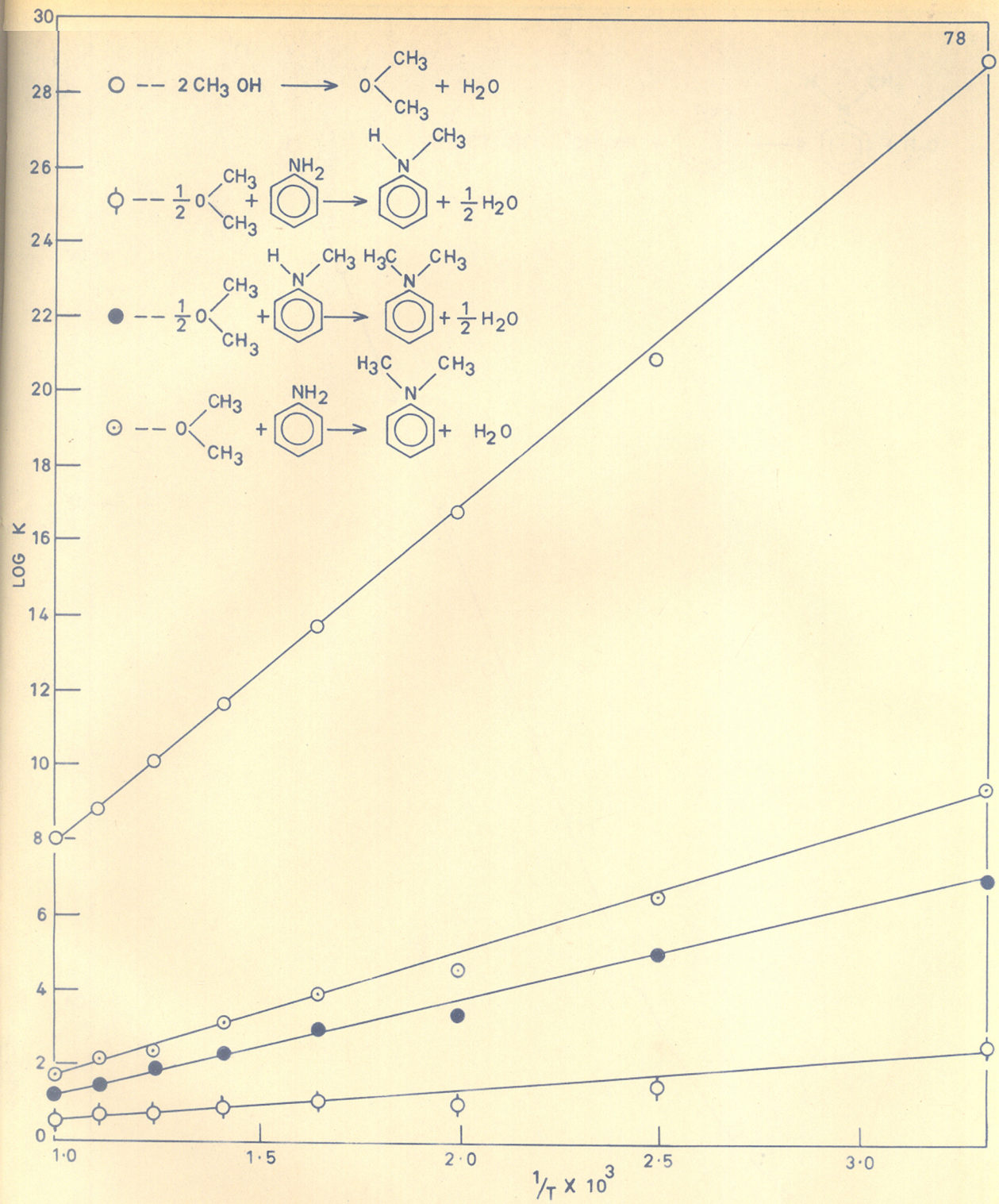

LOG K - $^1/_T$ PLOTS FOR REACTIONS (IV, V, VII & VIII)

FIG. - 13.

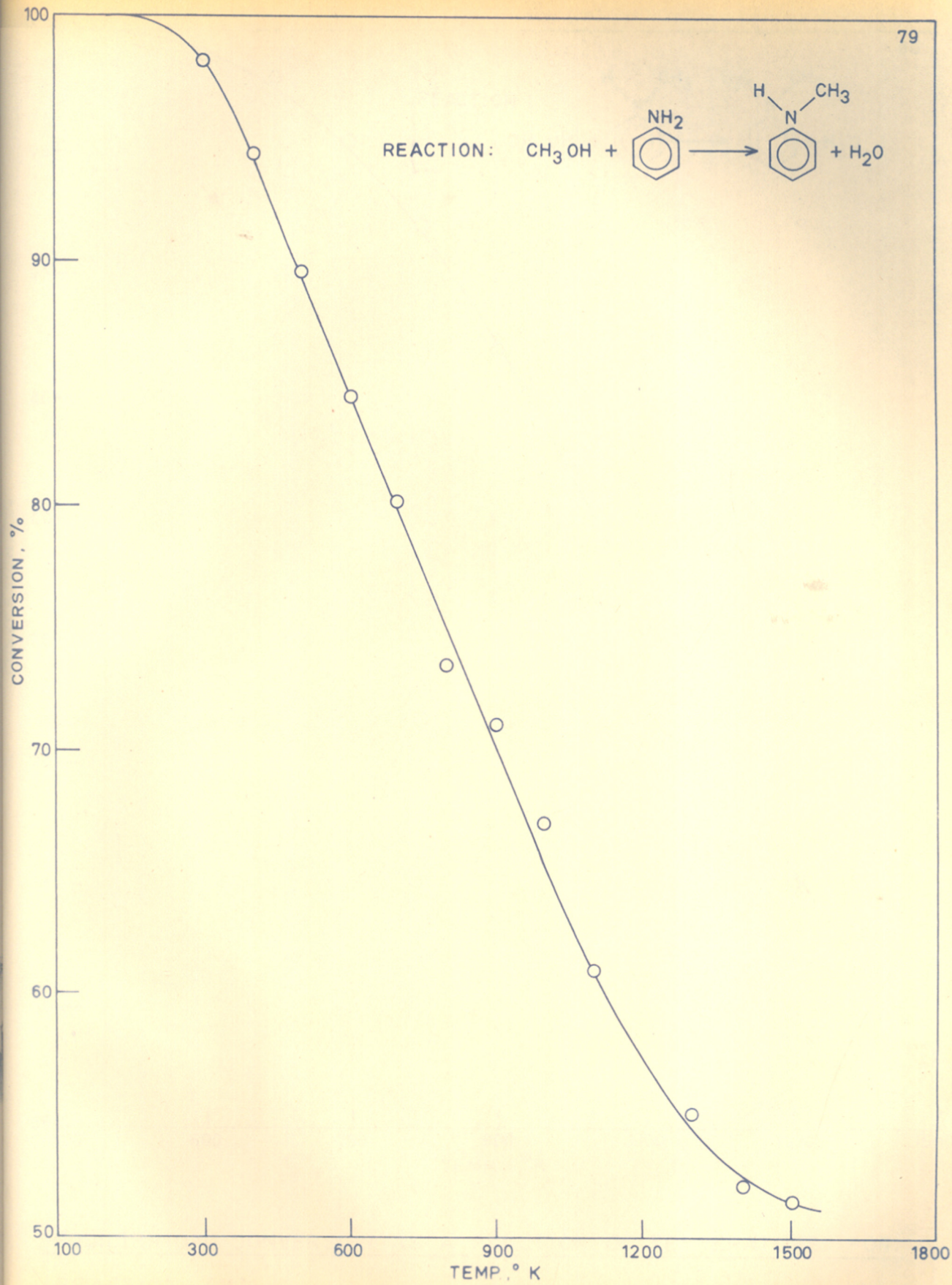

EQUILIBRIUM CONVERSION AS A FUNCTION OF TEMPERATURE FOR REACTION (I)

FIG - 14

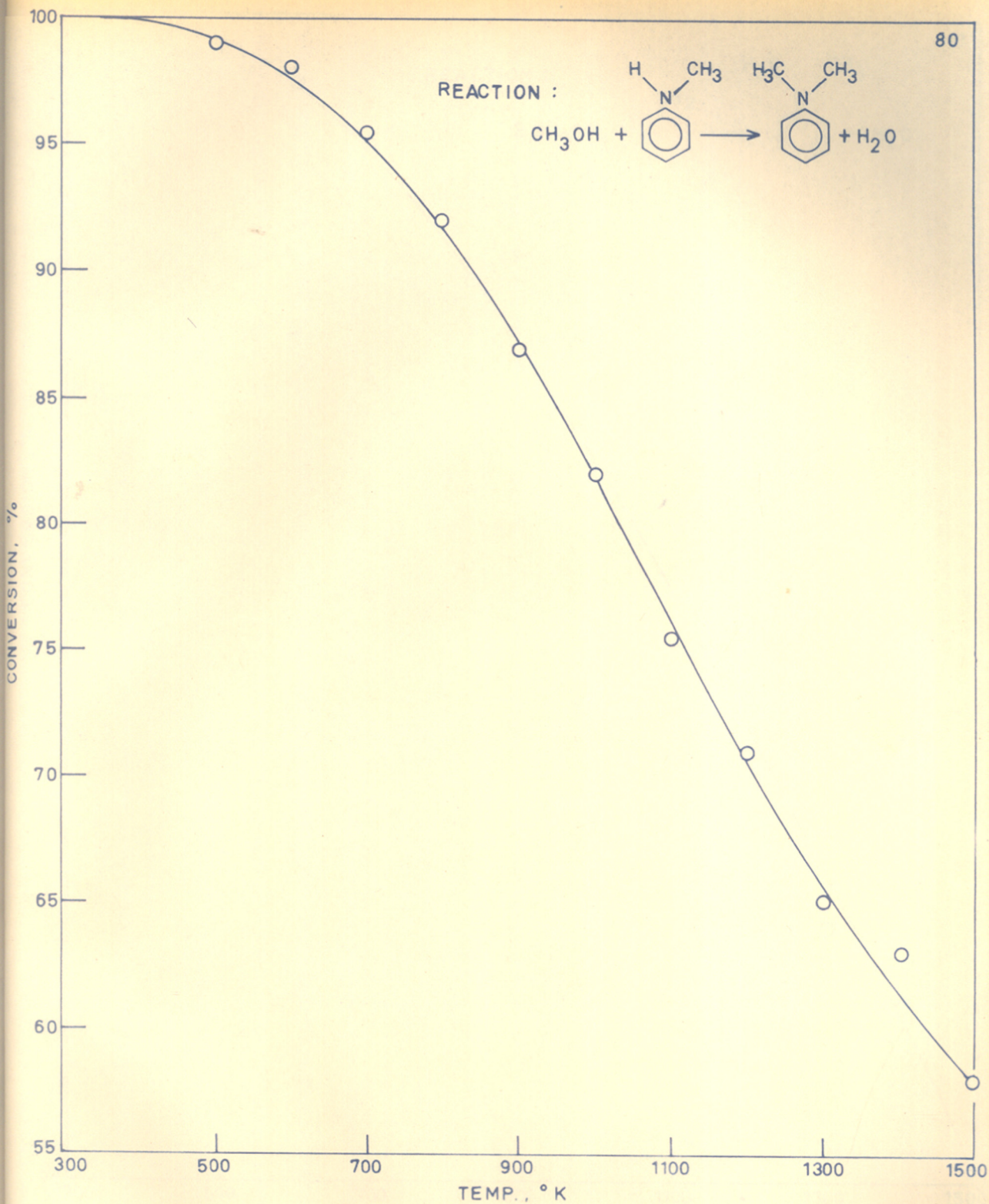

EQUILIBRIUM CONVERSION AS A FUNCTION OF TEMPERATURE FOR REACTION (II)

FIG. - 15.

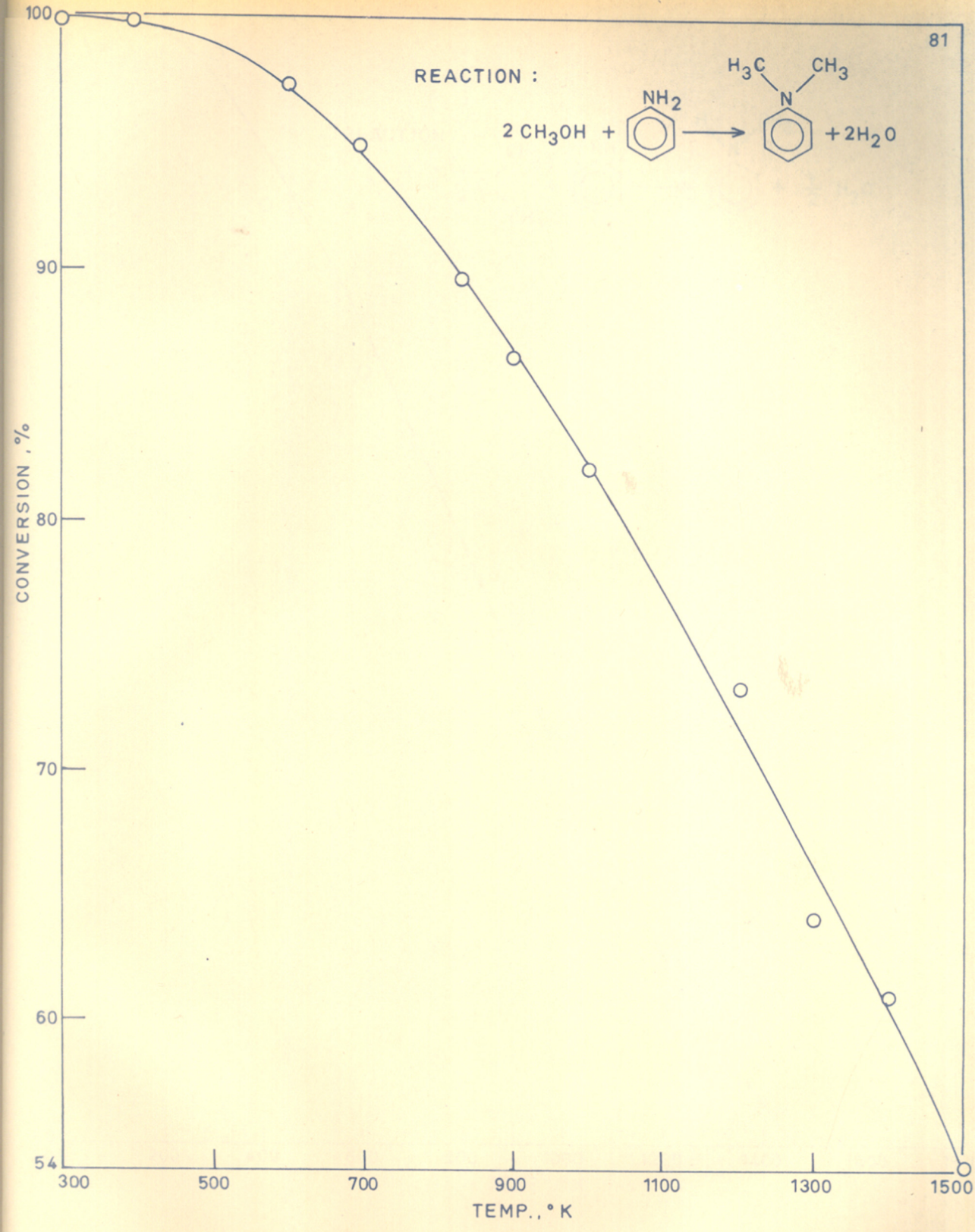

EQUILIBRIUM CONVERSION AS A FUNCTION OF TEMPERATURE FOR REACTION (III)

FIG. - 16.

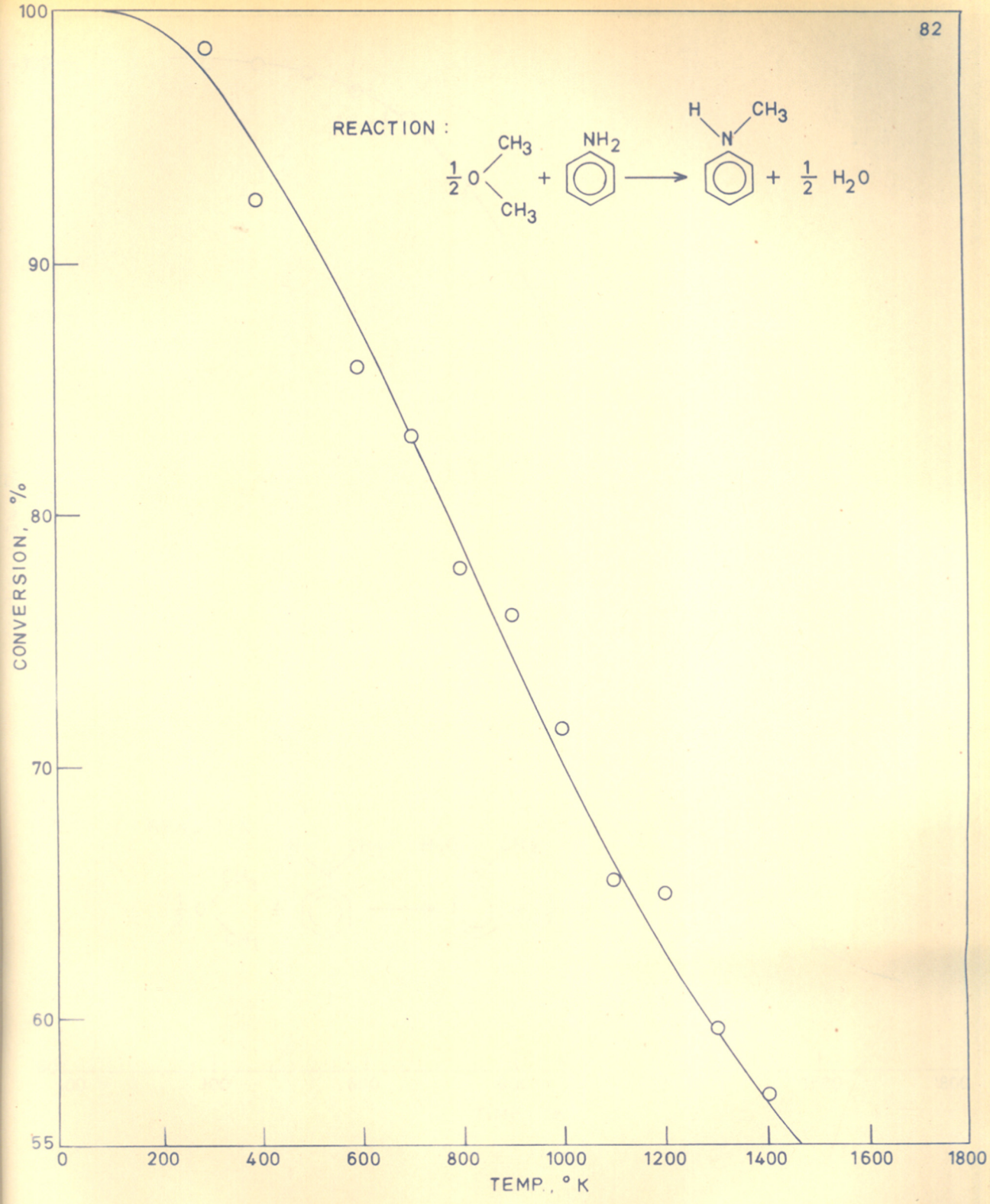

EQUILIBRIUM CONVERSION AS A FUNCTION OF TEMPERATURE FOR REACTION (V)

FIG.– 17.

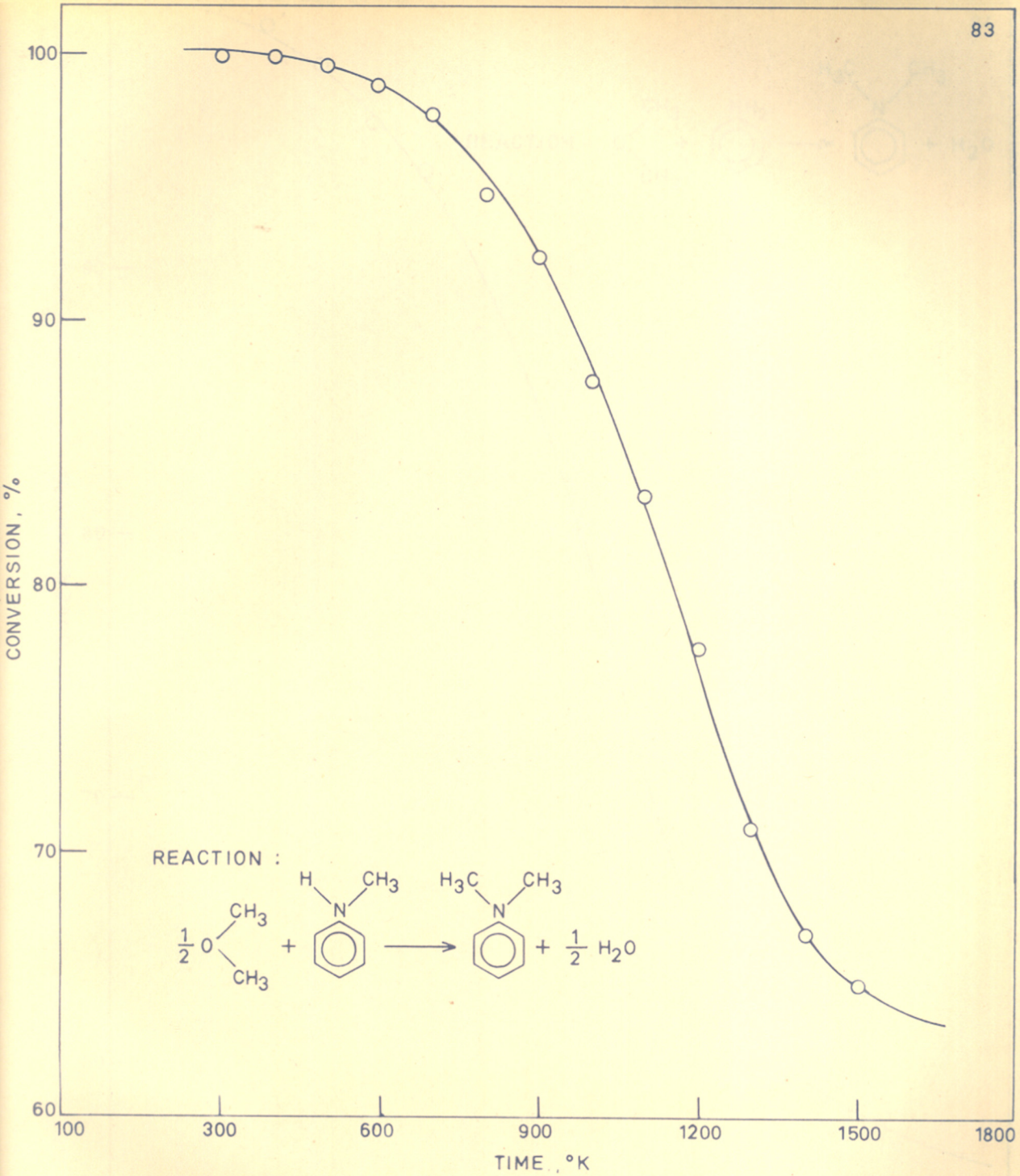

EQUILIBRIUM CONVERSION AS A FUNCTION OF TEMPERATURE FOR REACTION (VI)

FIG. - 18.

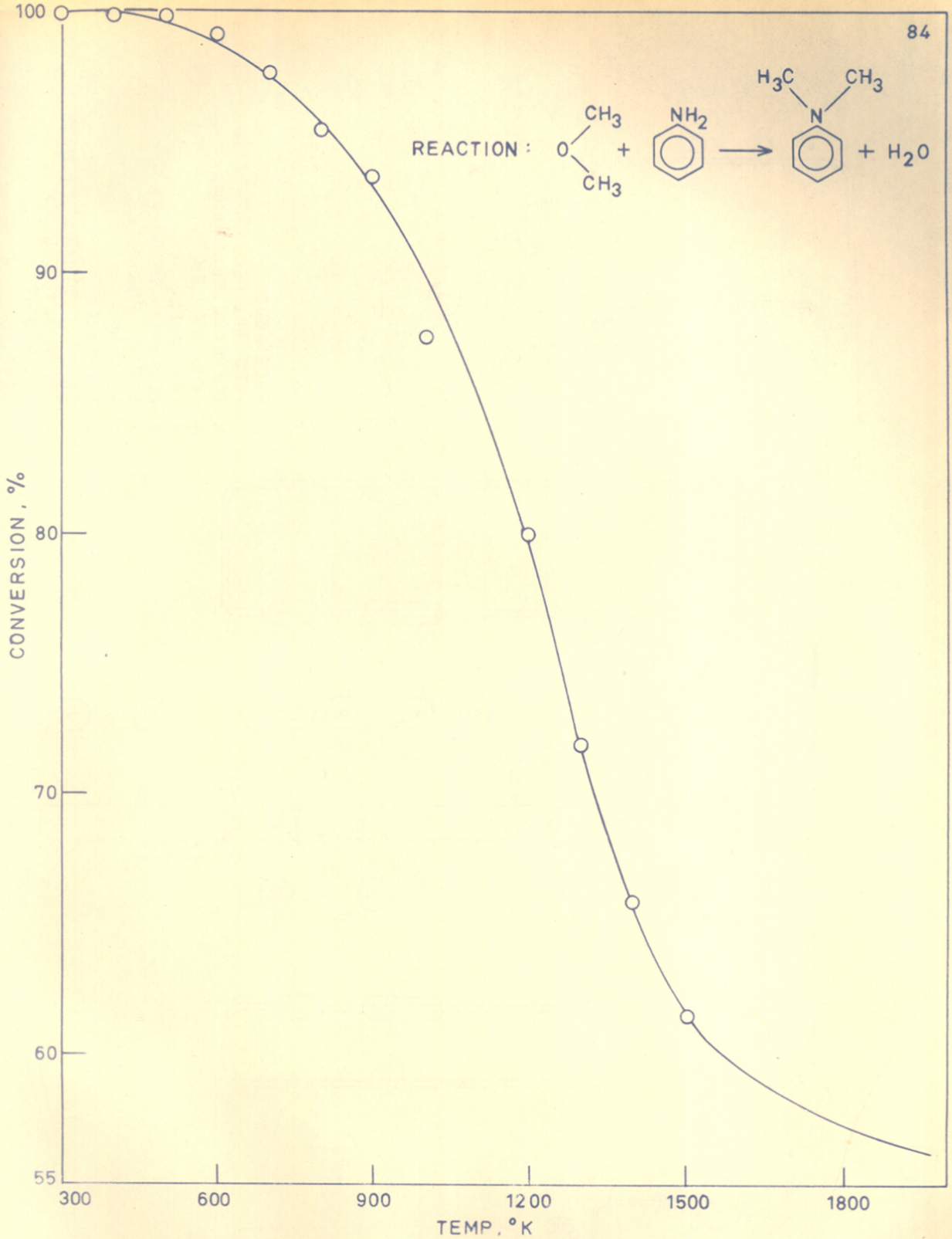

EQUILIBRIUM CONVERSION AS A FUNCTION OF TEMPERATURE FOR REACTION (VII)

FIG.–19.

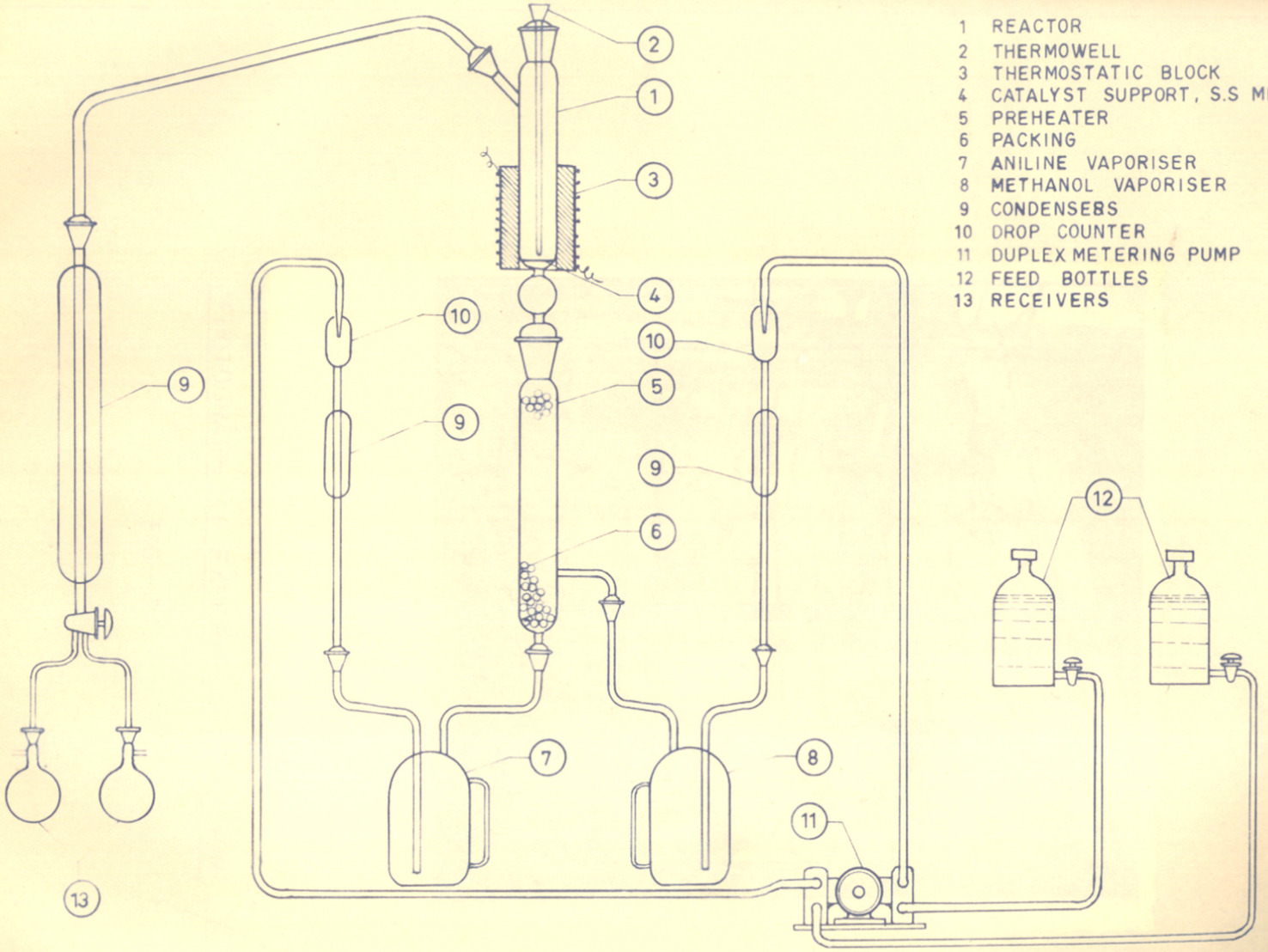

EXPERIMENTAL SET-UP

FIG. - 20

PHOTOGRAPH OF EXPERIMENTAL SET-UP

FIG. - 21.

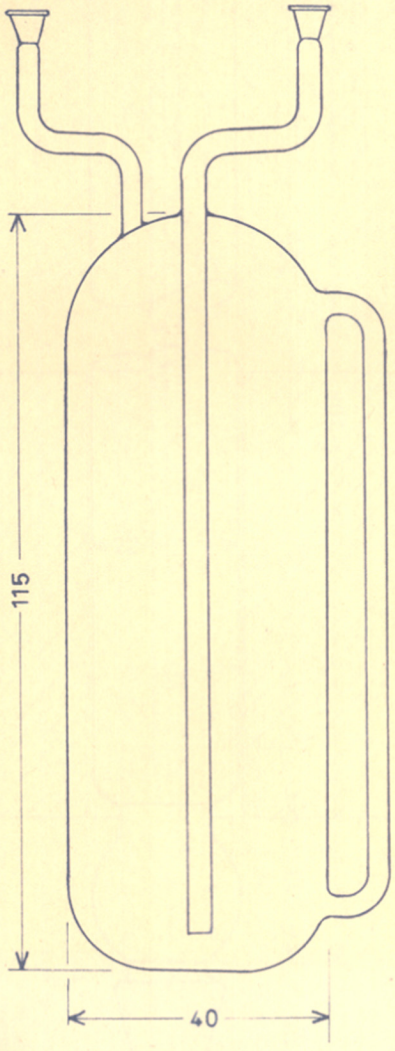

VAPOURISER

FIG.-22.

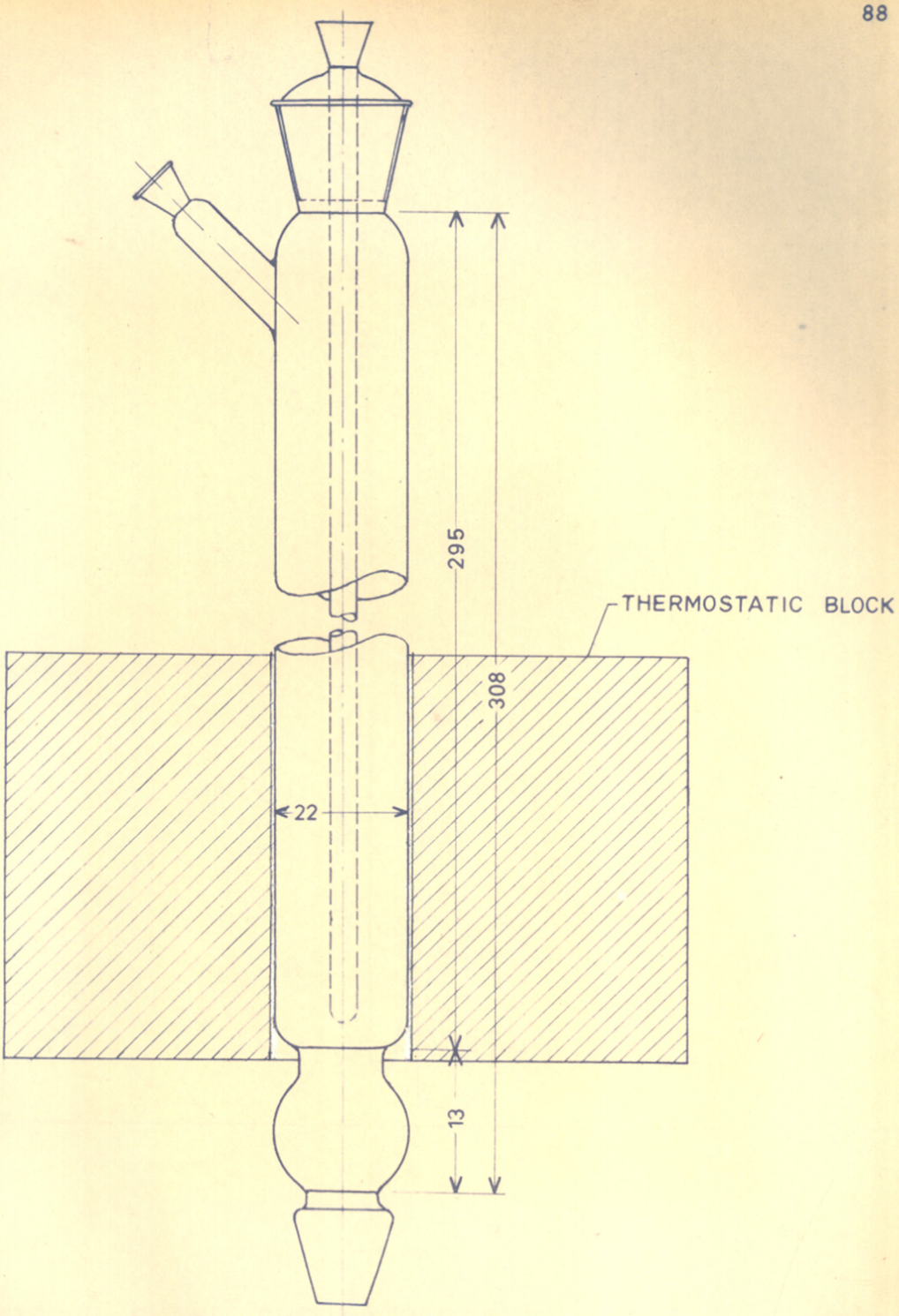

REACTOR

FIG.-23.

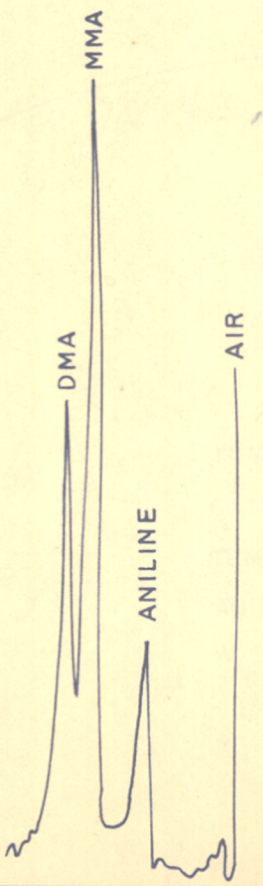

VAPOUR PHASE CHROMATOGRAPHY CHART

FIG.- 24

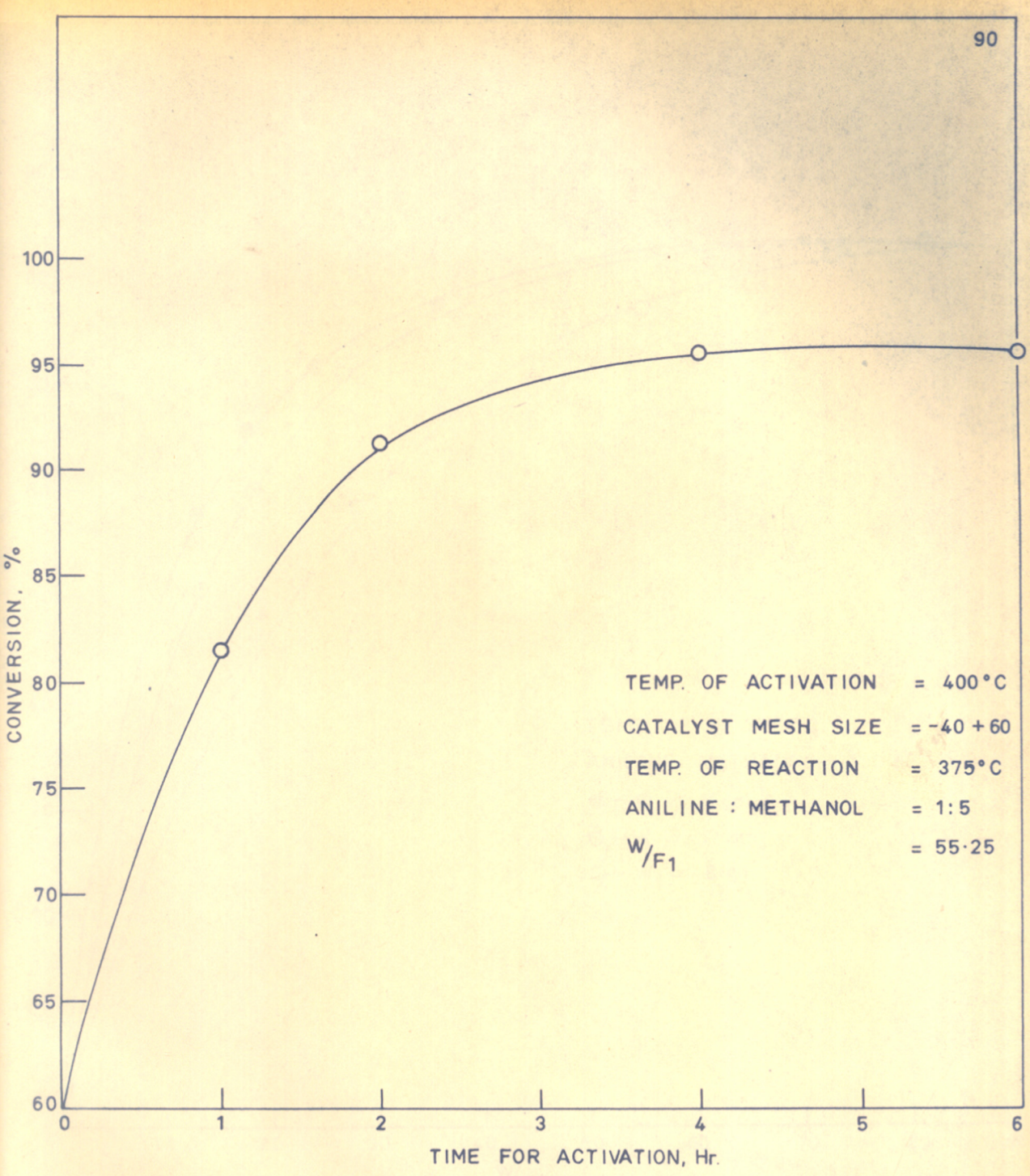

PLOT OF TIME FOR ACTIVATION VS. CONVERSION

FIG.- 25.

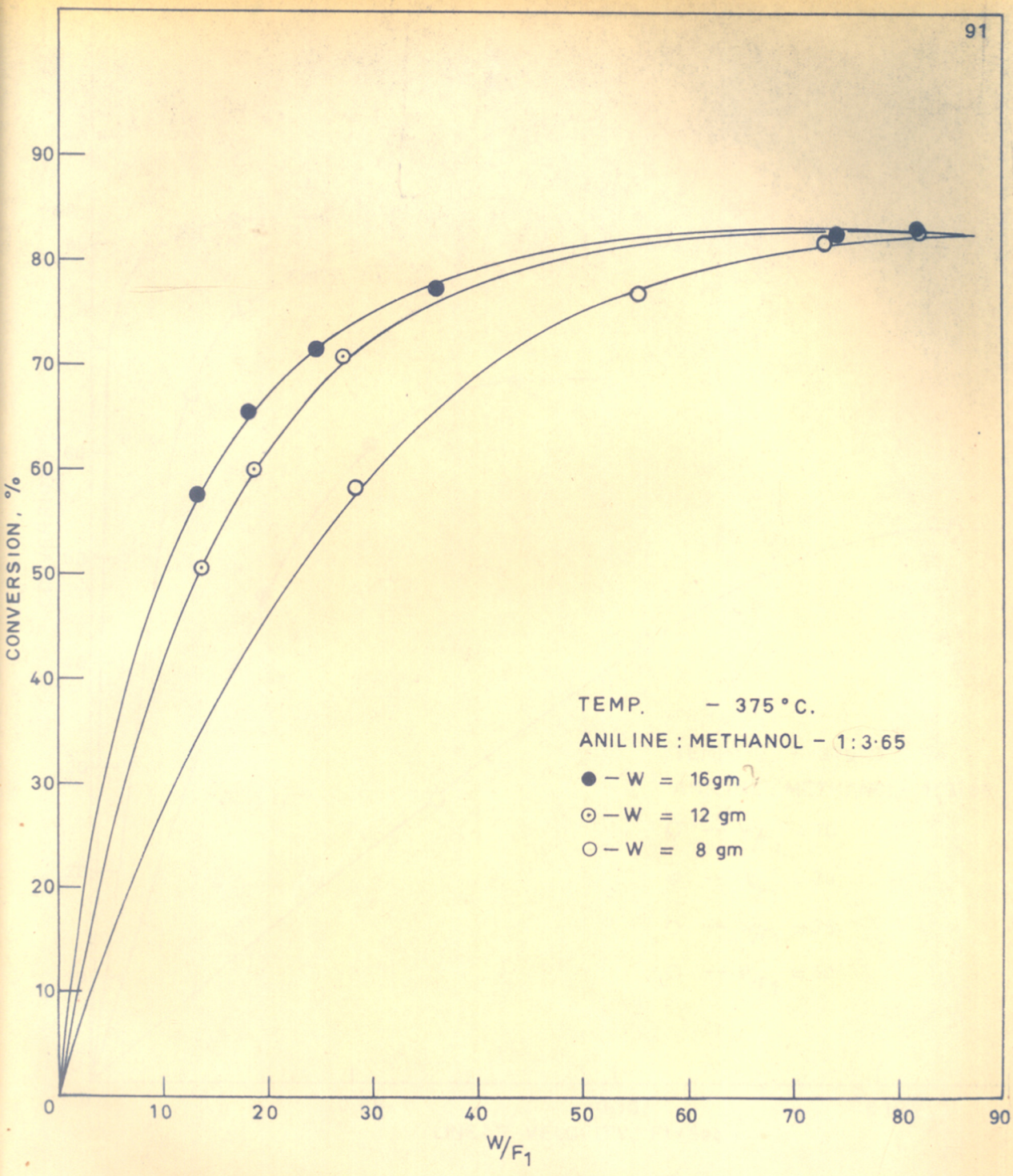

EFFECT OF MASS TRANSFER

FIG.-26.

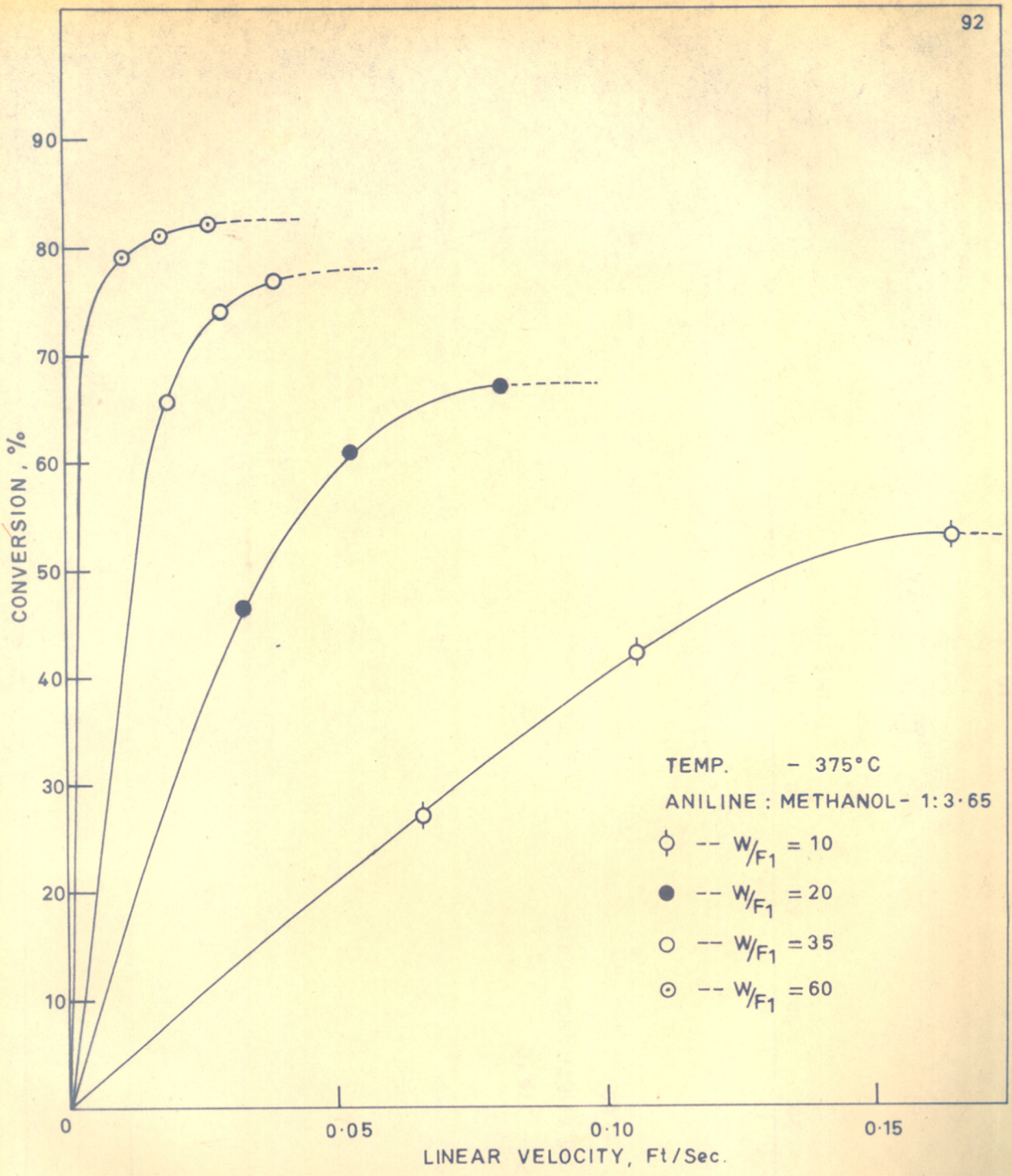

EFFECT OF MASS TRANSFER

FIG.- 27.

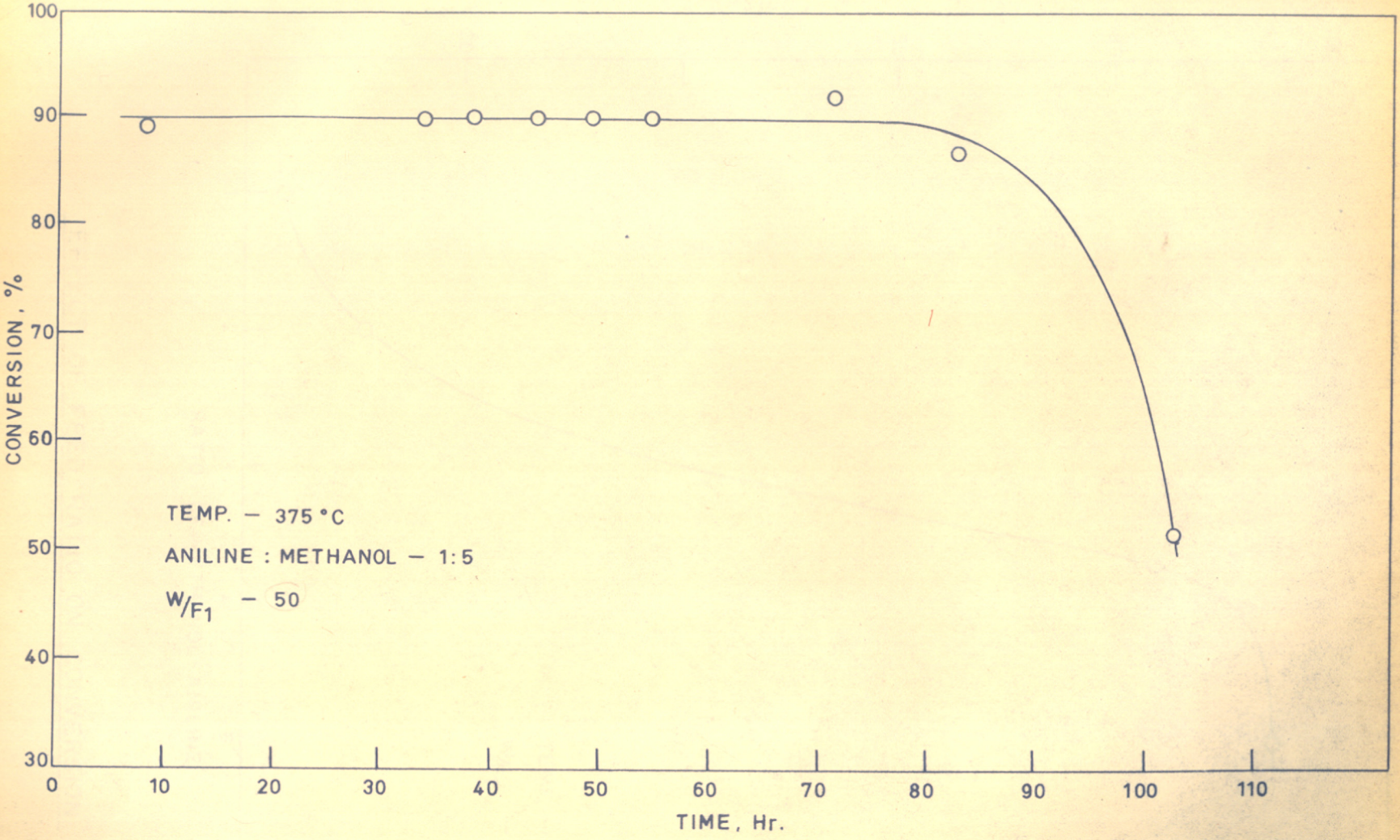

LIFE TEST

FIG.-28.

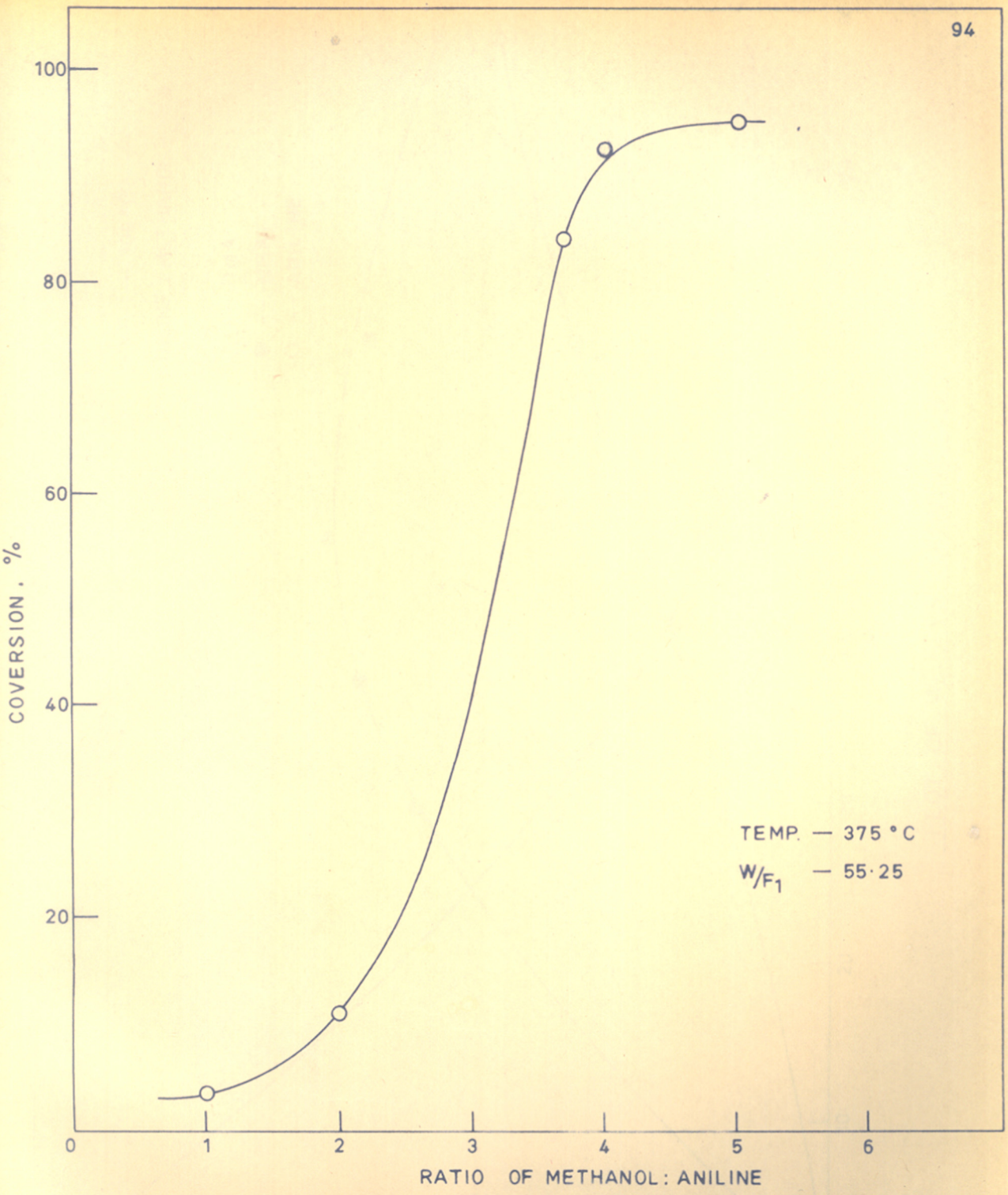

EFFECT OF FEED RATIO ON CONVERSION

FIG.- 29 .

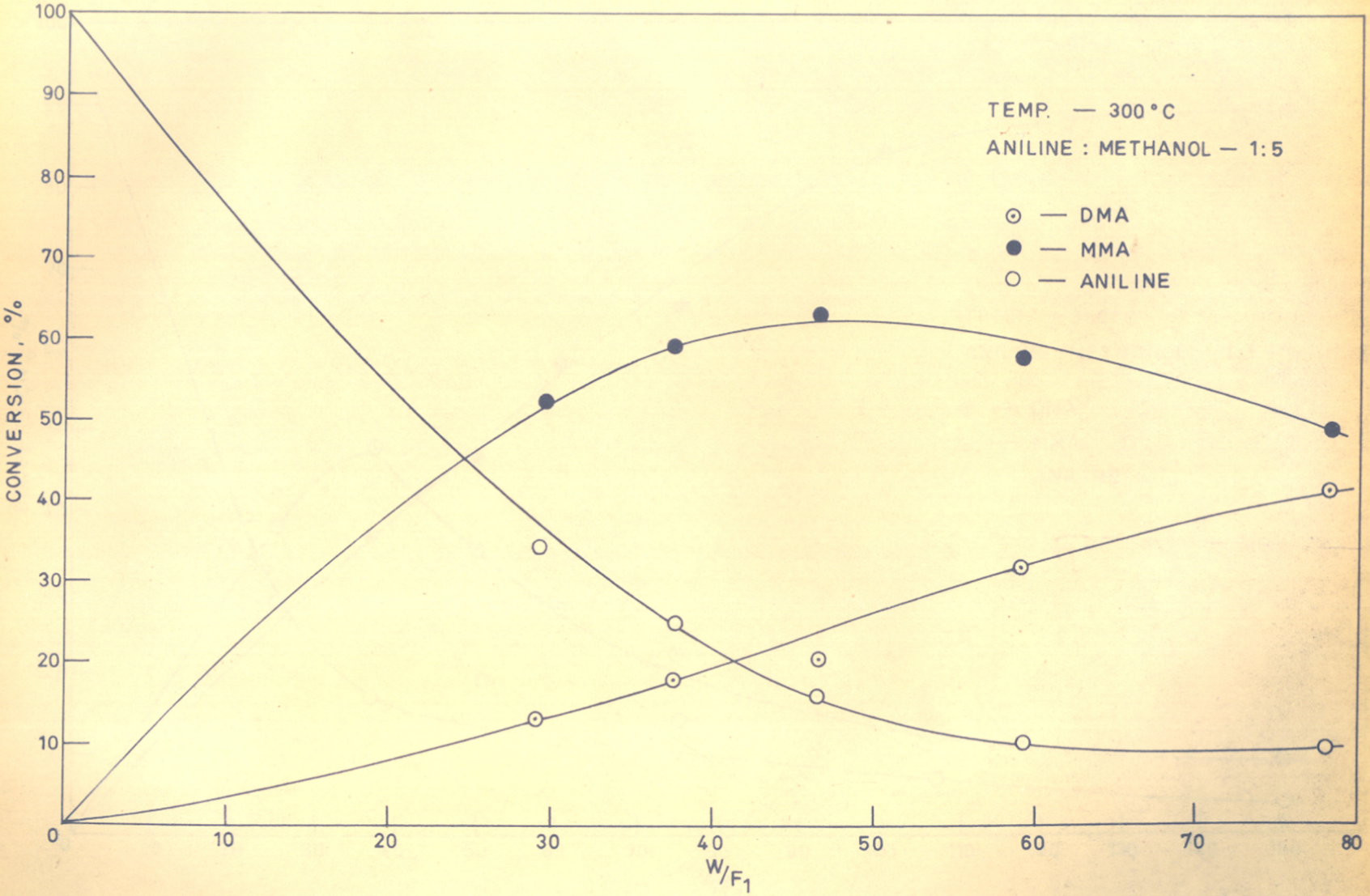

PLOT OF W/F_1 VS. CONVERSION

FIG.-30.

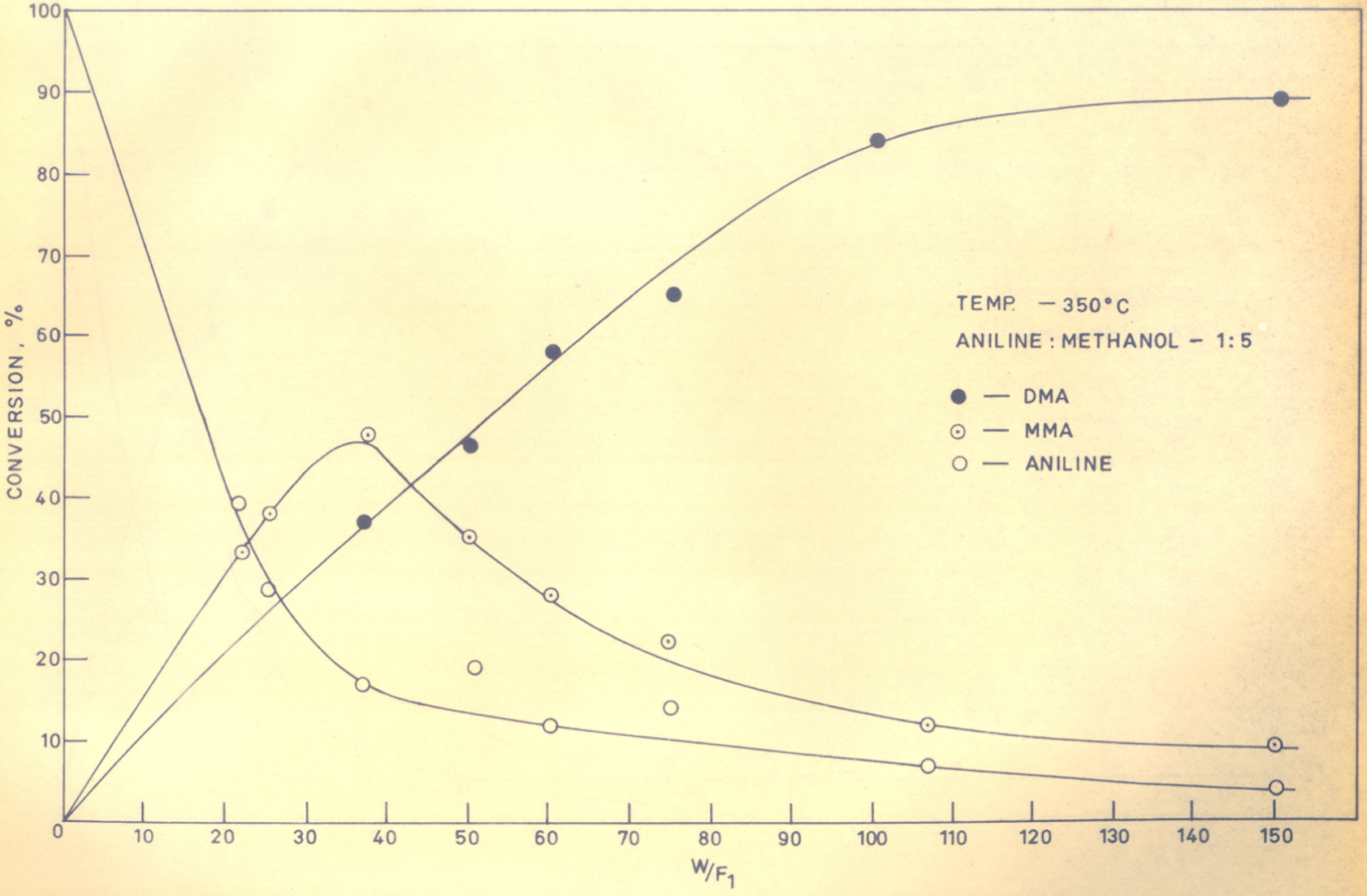

PLOT OF W/F_1 VS. CONVERSION

FIG. - 31.

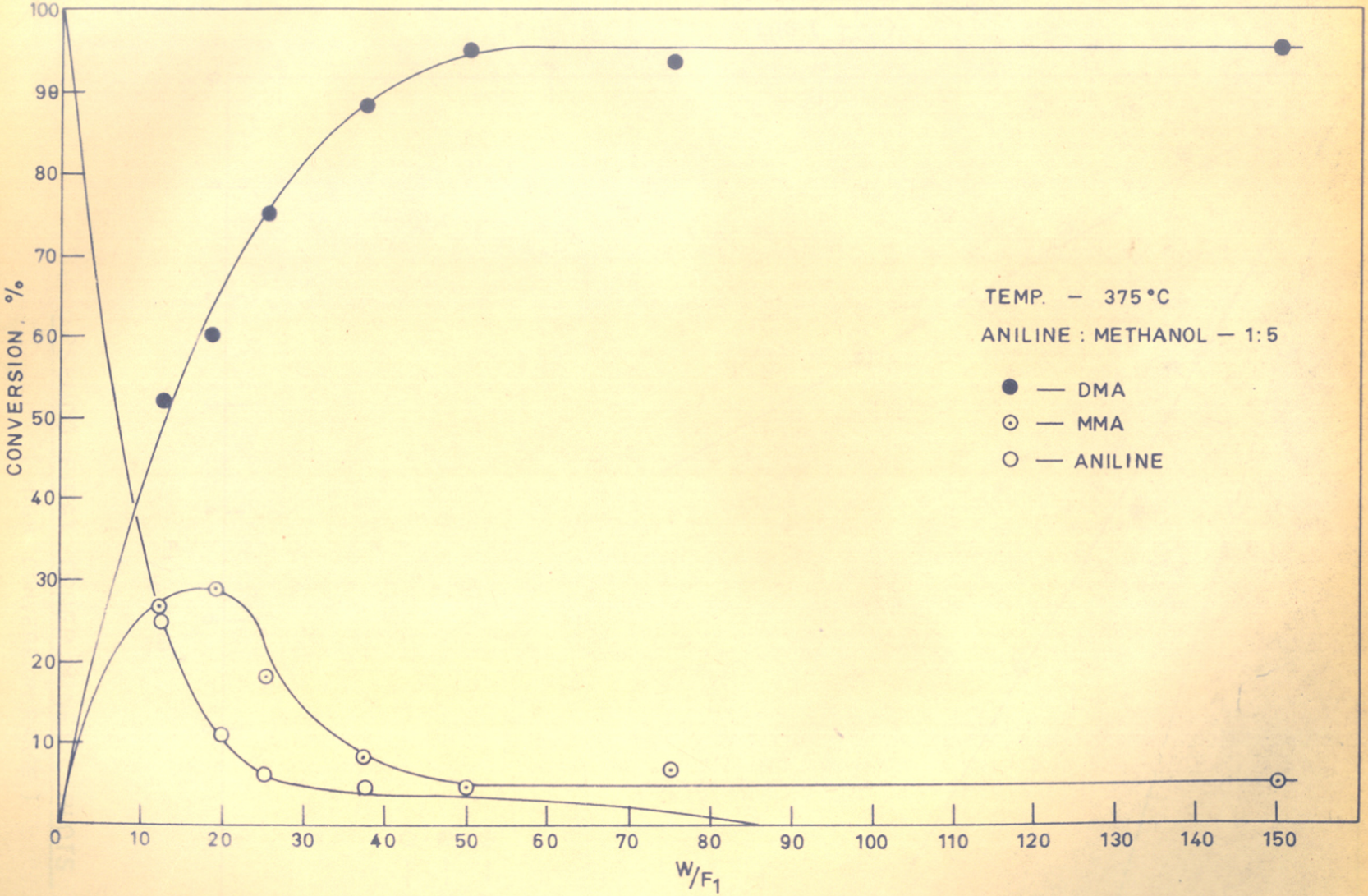

PLOT OF W/F_1 VS. CONVERSION

FIG.-32.

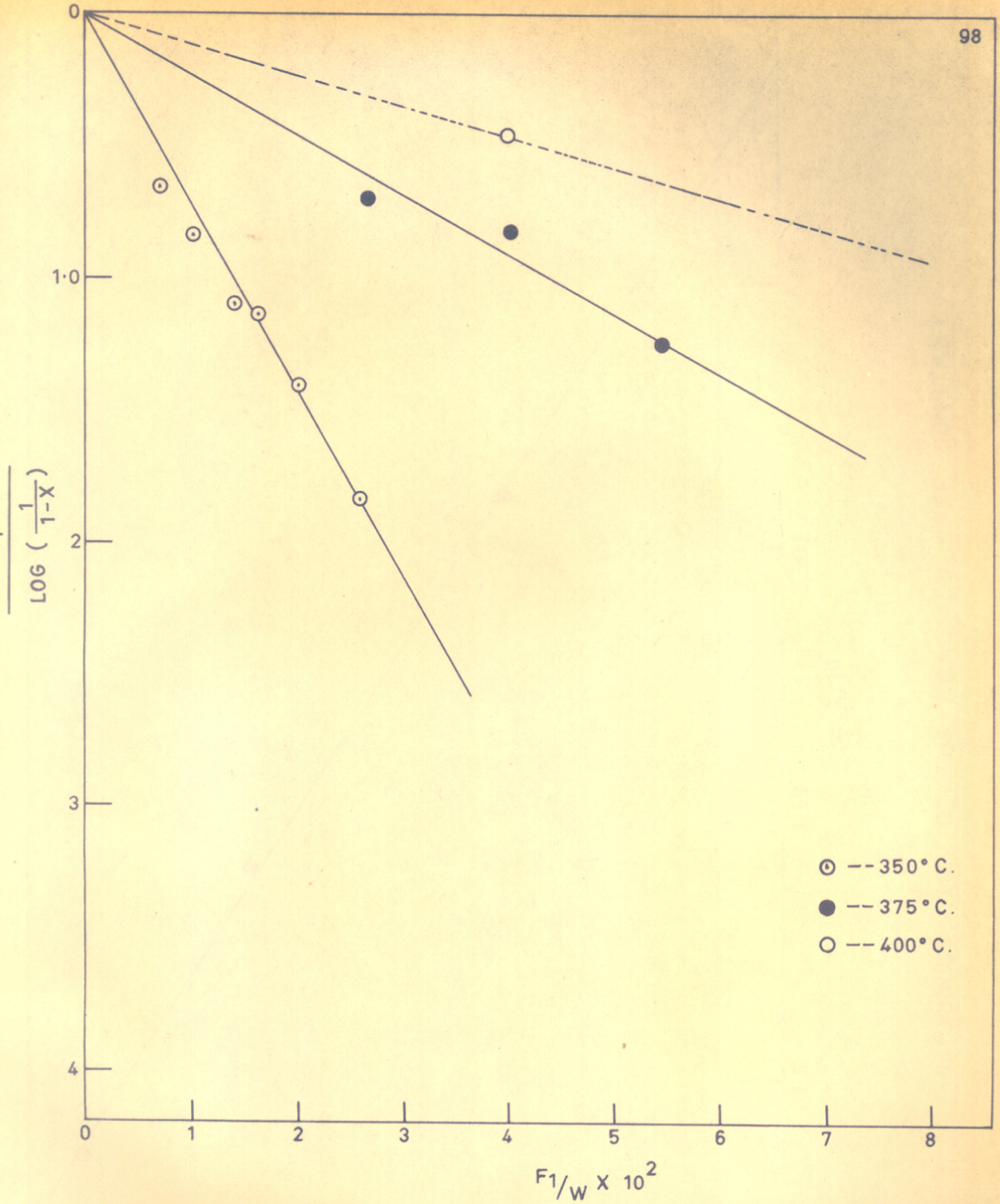

PSEUDO-FIRST ORDER KINETIC PLOTS

(HIGH CONVERSION RANGE)

FIG.- 33.

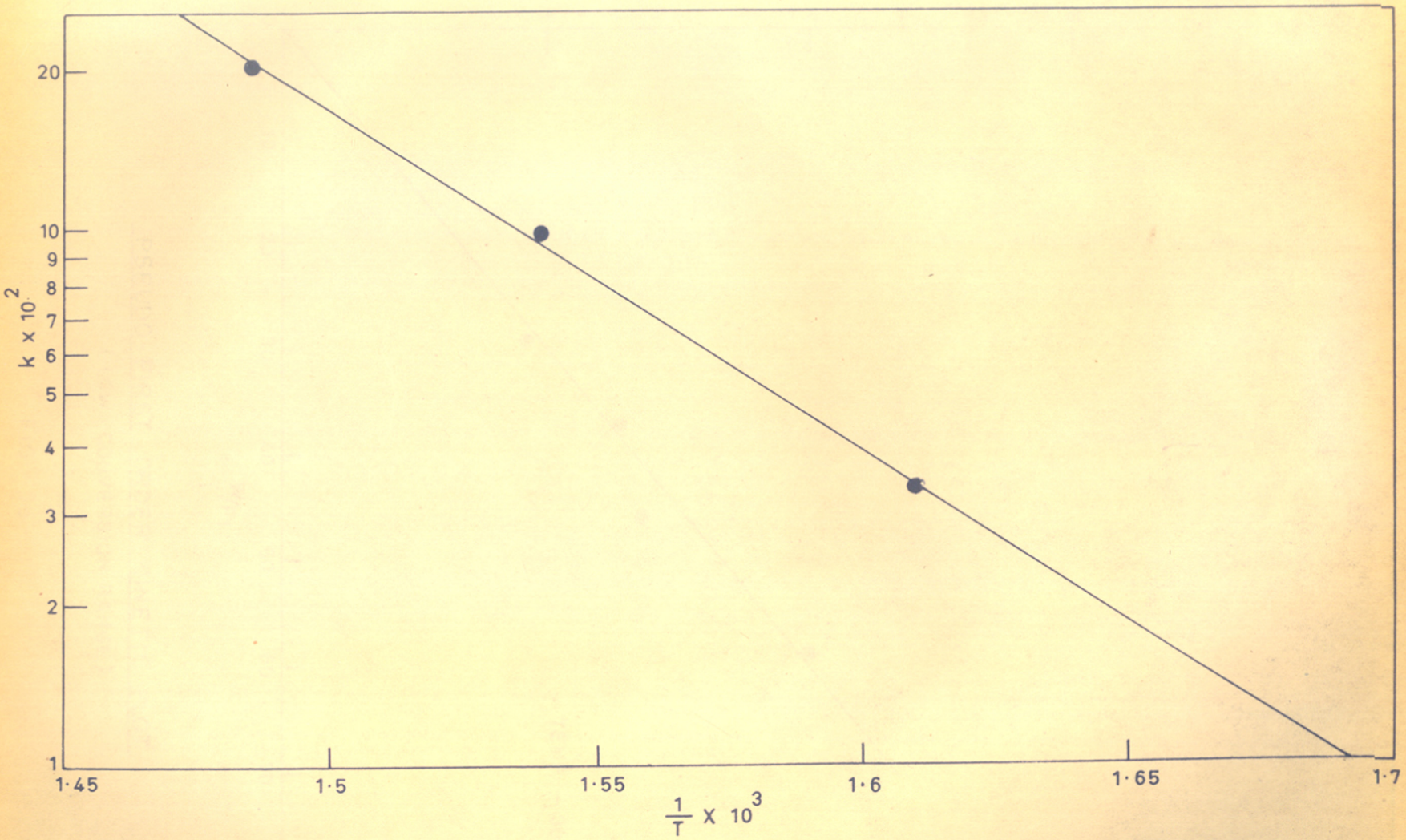

ARRHENIUS PLOT OF THE REACTION RATE CONSTANT

FIG.- 34.

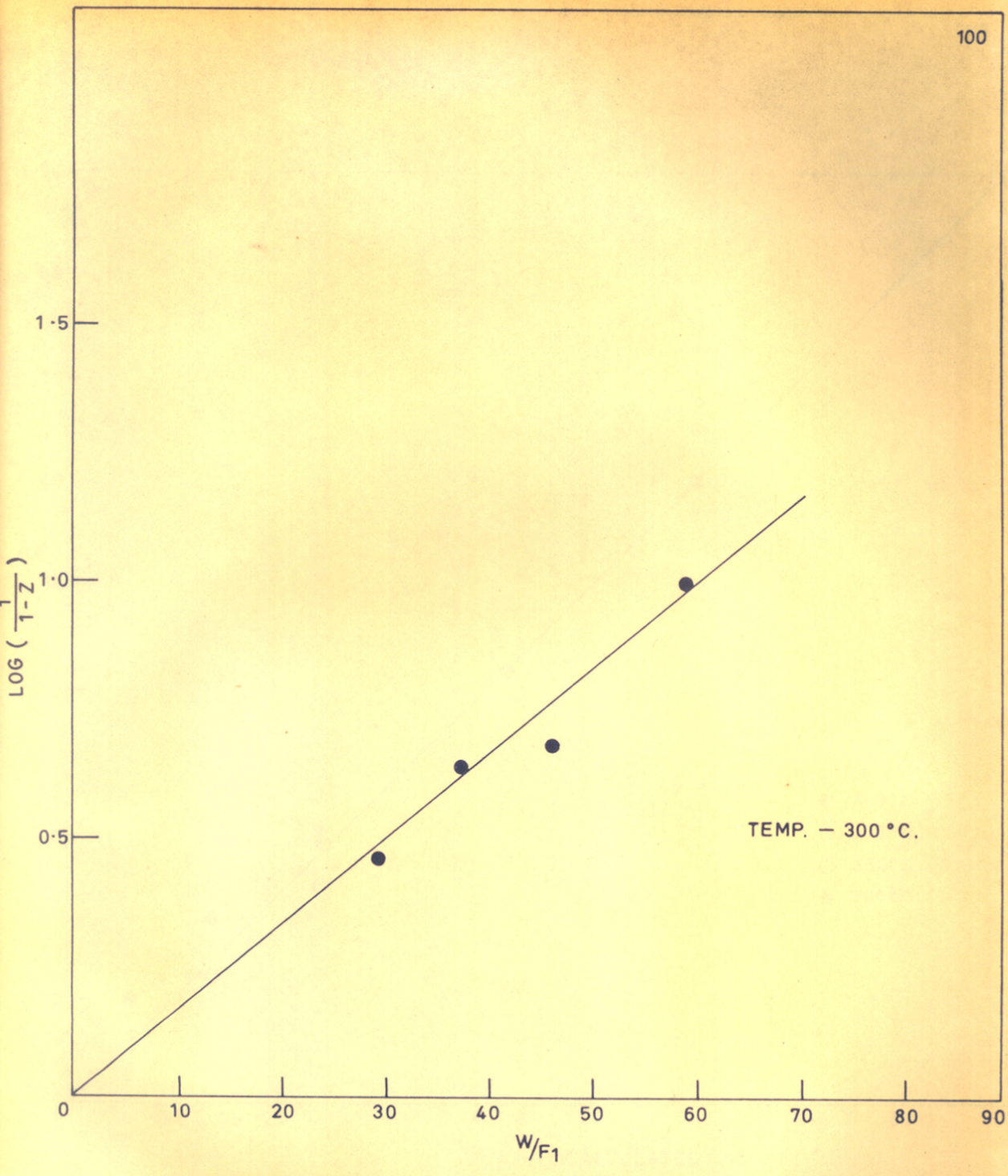

PSEUDO-FIRST ORDER KINETIC PLOT

(LOW CONVERSION RANGE)

FIG.-35.

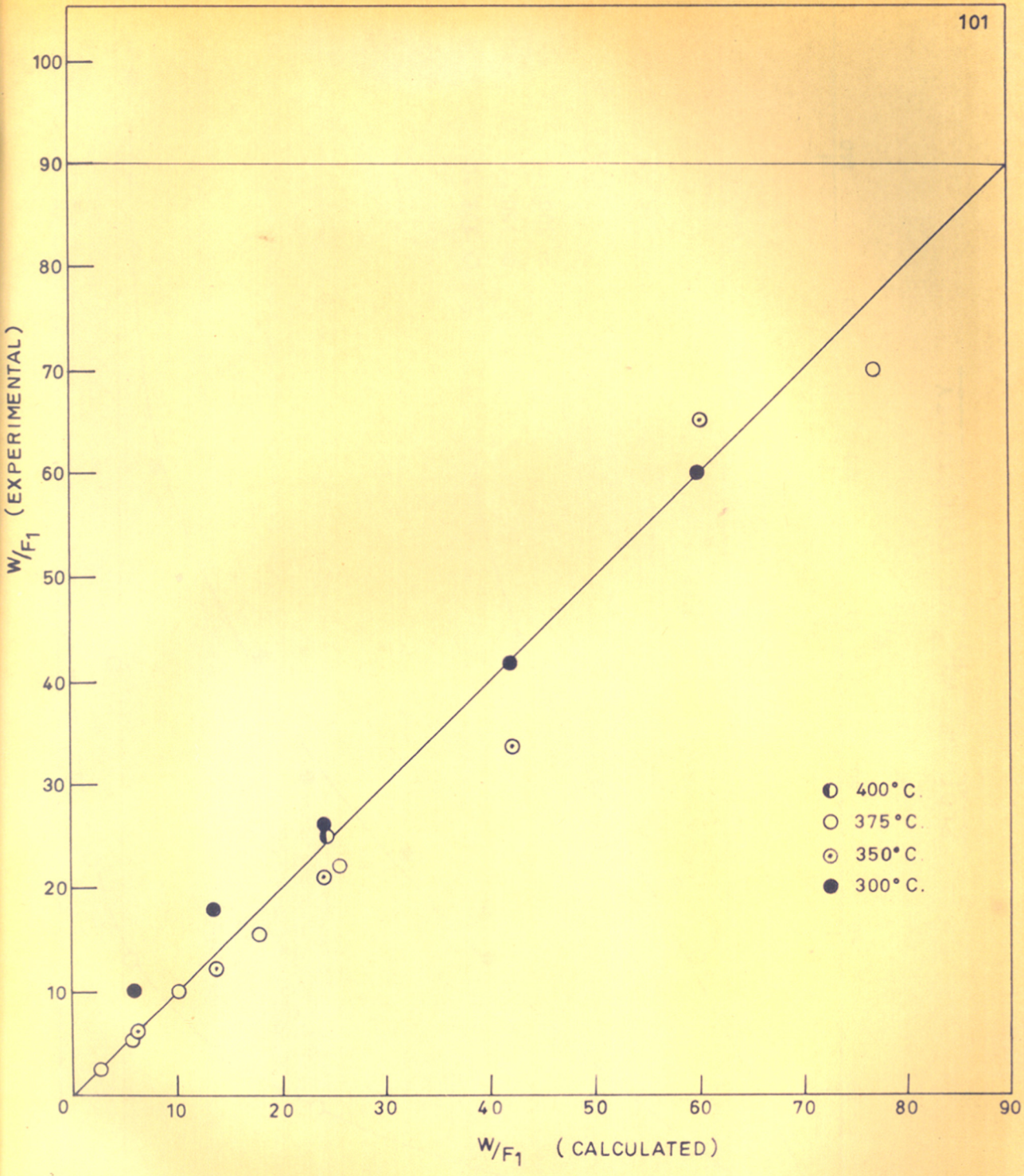

COMPARISON OF EXPERIMENTAL VALUES WITH THOSE CALCULATED BY EQUATION 4.

NOTE - EXPERIMENTAL VALUES HAVE BEEN TAKEN FROM THE CURVES OF FIGS. 30, 31, 32.

FIG. - 36

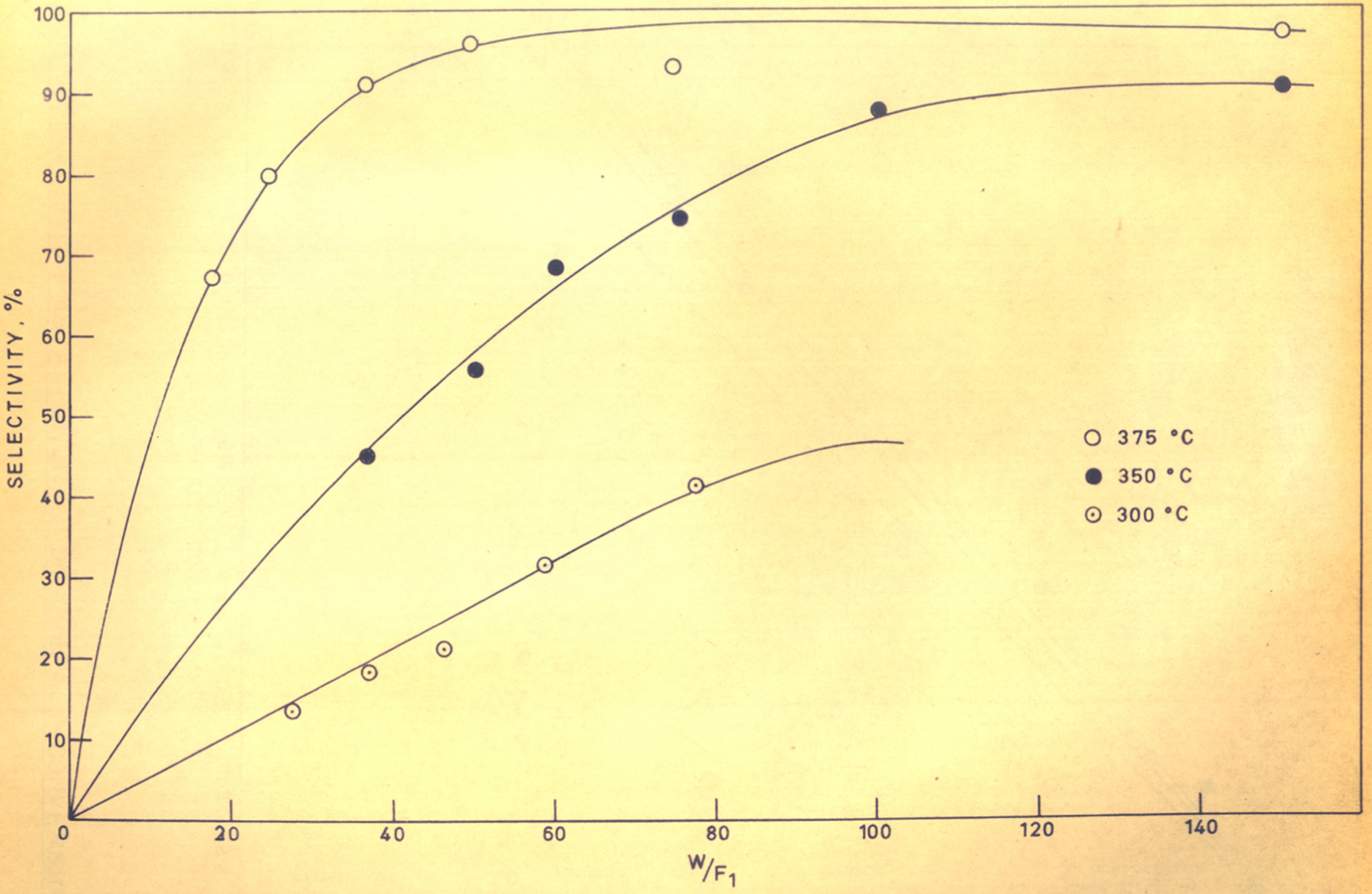

PLOT OF W/F_1 VS. SELECTIVITY

FIG.-37.

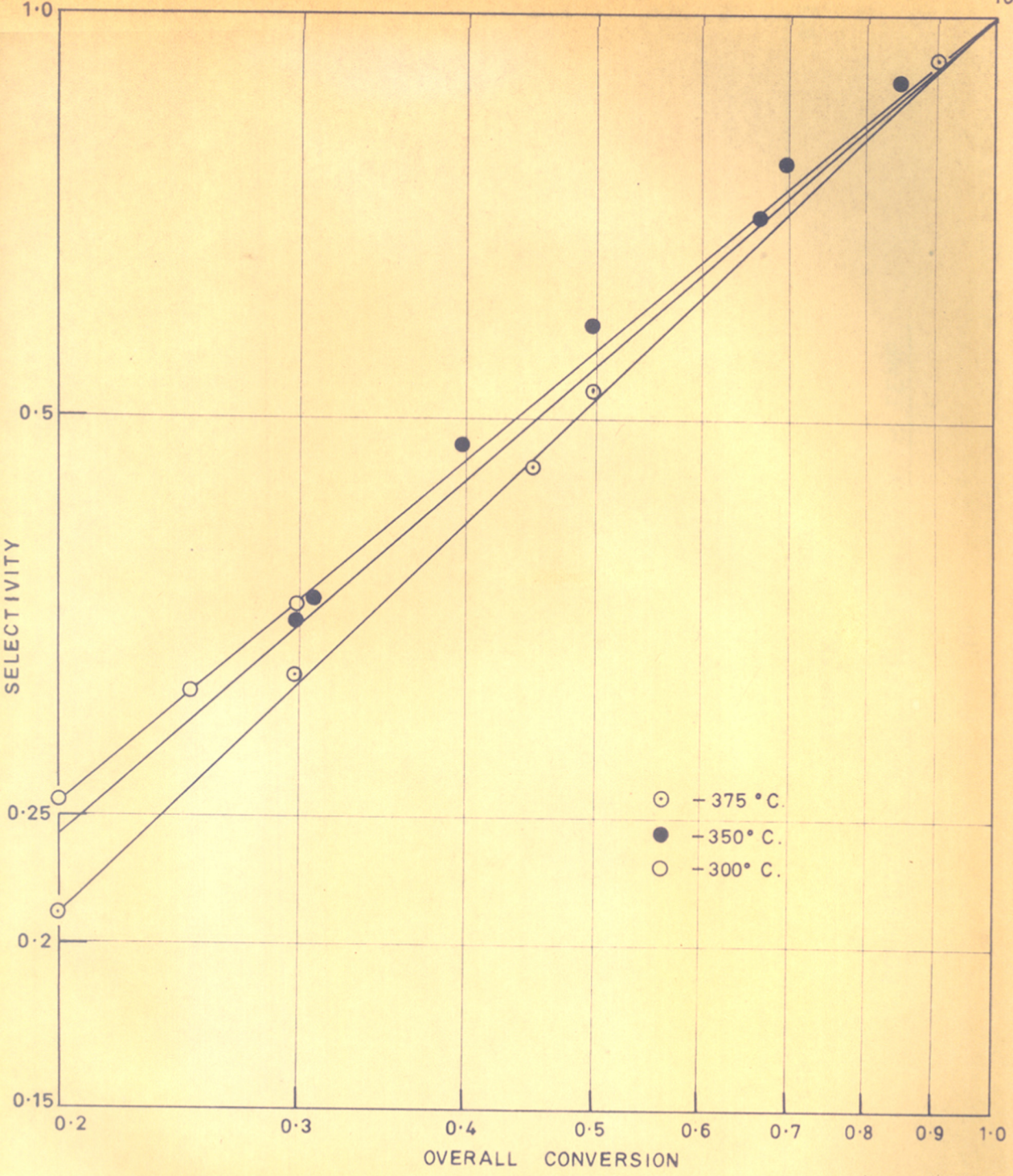

DMA SELECTIVITY AS A FUNCTION OF OVERALL CONVERSION

FIG. – 38.

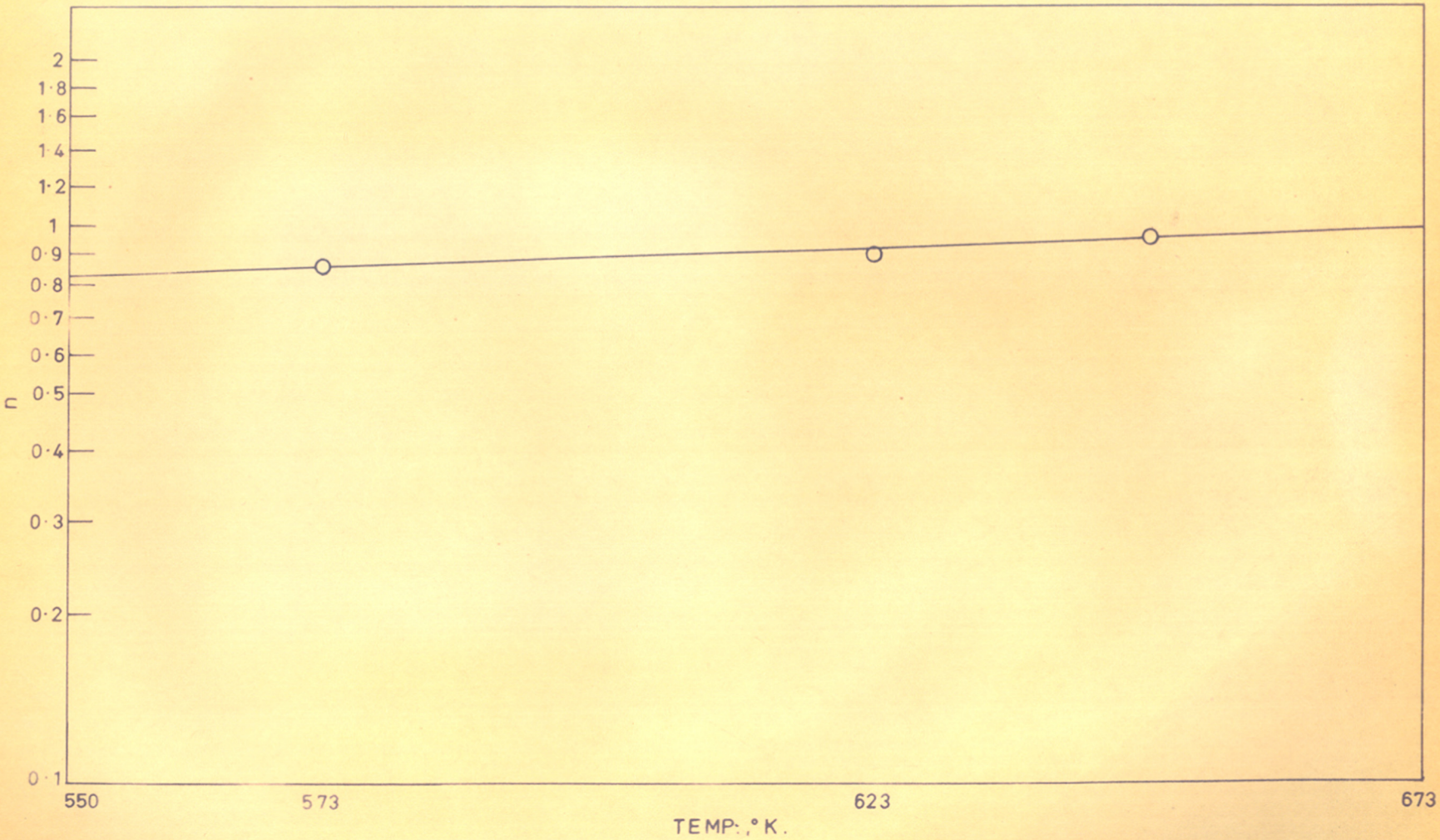

CORRELATION OF n (EQUATION 9) WITH TEMP.

FIG - 39.